acta physica slovaca vol. 64 No. 1, 1 – 56 **February 2014**

OCEAN MIXING BY WAVE ORBITAL MOTION

Malek Ghantous*,[1,2] and Alexander V. Babanin[2]
[1] *LEGOS, CNRS/University of Toulouse, Toulouse, France*
[2] *COEST, Swinburne University of Technology, Melbourne, Victoria, Australia*

Received 31 August 2014, accepted 15 October 2014

Improvements in numerical ocean models and more and better observations have made the gaps between the two all the more apparent. In a recent resurgence in the study of turbulence due to wave orbital motion, some scholars have sought to address part of the problem by proposing the mechanism as an important missing part from vertical mixing models. Yet the subject remains contentious. This review is an attempt to bring together in one place the main results and insights from almost a century of scholarly discourse on the subject, demonstrating the breadth of ideas therein, as well as highlighting some of the outstanding problems.

DOI: 10.2478/apsrt-2014-0001

PACS: 92.10.Fj, 92.10.Hm, 92.10.Lq

KEYWORDS: Wave-induced turbulence, Wave-induced mixing, Ocean waves, Ocean mixed layer, Coupled models, Turbulence, Turbulent mixing, Ocean boundary layer, Wave-turbulence interaction

Contents

*E-mail address: malek.ghantous@legos.obs-mip.fr

1 Introduction

Turbulence may be characterised as a chaotic, eddying fluid flow facilitating the transfer and mixture of fluid properties such as momentum and heat throughout the fluid. Though the subject is old, with many of the concepts being formalised in the late 19th century [Boussinesq, 1877, Reynolds, 1883], turbulence has proven remarkably resilient to analytical approaches, frequently being referred to as the last unsolved problem in classical physics. Despite decades of improvements in computer models, experiments, observations and theory, turbulence remains a subject where definitions are rarely universal and our understanding poor. This review paper is dedicated specifically to the turbulence generated due to mechanical motion of water along the sub-surface orbital motions of surface gravity waves, and the mixing generated by this turbulence.

When it comes to turbulent mixing in the ocean the above problems are accentuated by the difficulty of making good observations in the open ocean. Contamination by the measuring instruments interacting with the flow, sometimes extreme weather and ocean conditions and the never-ending movement of surface waves, internal waves and currents, make measuring anything difficult, and separating one phenomenon from all the others in any measurement is often impossible without an ideal—and rare—instrumental setup.

Numerical models can be almost as much of a hindrance as a help, since so many assumptions are made when developing them, and they all need to be tuned to some extent to observations. What's more, they are frequently contradictory, calculating quite different rates of mixing. Indeed, sometimes the better performing models are the less sophisticated ones, indicating that our knowledge of the physical processes involved is incomplete. That the most sophisticated models, which purport to represent the physics as closely as can reasonably be done in a large-scale ocean model, should perform so poorly at times indicates that some process, perhaps several, is missing from ocean mixing models—as noted by Qiao and Huang [2012], mixing in the extra tropics in summer is in particular poorly predicted. Certainly there are processes which are difficult to predict and to parameterise, such as internal waves, which are known to affect mixing when they break. Turbulence generated by the orbital motion of surface gravity waves, which are easier to predict, is a good candidate for filling the gap, and we may be encouraged that the symmetrical problem of predicting dissipation of ocean swell might be solved at the same time. But of the many processes that serve to mix oceanic waters this one in particular has yet to gain complete acceptance among the oceanographic community.

It is not entirely obvious why this should be so. While the subject is not new, and despite the existence of theoretical, experimental and observational work on it, it has been largely ignored by the oceanographic community for the past half century or so, and many still feel that the mechanism is somewhat implausible, or at least negligible in the context of ocean mixing. Babanin et al. [2012] alludes to one possible reason for this: the success of potential wave theory, especially from the 1960s, in explaining a wide variety of wave phenomena. One may occasionally even hear the argument from scholars that waves, since they are irrotational, cannot produce turbulence. This view is doubly mistaken—firstly real wave motion is not potential, since water is, like all real fluids (quantum superfluids aside) viscous. Secondly, this misses the point, and appears to stem from a misreading of a fundamental result of fluid mechanics, which states that in a fluid with no viscosity an irrotational flow will never develop vorticity. But this says nothing about how a potential flow will respond to a pre-defined vorticity. As long as vorticity is imposed on a flow, even without viscosity, any shearing motion, even an otherwise irrotational one, can stretch the vortex lines. This gives a mechanism for generation of turbulence via the amplification of vorticity.

The argument that the effect is so small that it may be ignored is on firmer ground. Although there is now plenty of evidence which suggests otherwise, we are far from an accurate understanding of how wave orbital motion generates turbulence and its role in the ocean. Our aim in this review is to gather the main results from the published work we are aware of and to put it together in a coherent way so that researchers working in the field—both newcomers and old hands—will be able to avoid making some of the same mistakes, and to build on the preceding work. We hope that this will enable future efforts to progress our knowledge of the phenomenon and also to improve the way it is modelled. As is usual enough with nature, knowledge of more than one field is often necessary to understand it. In this case a knowledge of both surface gravity waves and turbulence is necessary, and since they are both immense subjects it is frequently the case that experts in one are not experts in the other. This has led to some unorthodox approaches which, while sometimes ingenious, and always very useful, are not always grounded in solid physical reasoning. We have of course fallen into this trap ourselves, and so it is without judgement that we attempt to identify inconsistent or incorrect approaches to the physics with the expectation that those from one field or the other will gain from this knowledge just as we have.

Before we go further we should clarify our terminology. Previously, "wave-induced turbulence" referred almost exclusively to turbulence generated by breaking surface waves, or whitecapping. Here when we refer to turbulence generated by wave breaking we say so explicitly, preferring to reserve the term "wave-induced turbulence" as a generic one. While the term could be most justifiably used to group together all forms of turbulence due to surface gravity waves (here internal waves are implicitly left out), we have decided to let context be the decider when only one is meant—in this review that means turbulence generated by wave orbital motion, not including breaking. We label mixing due to Langmuir circulation explicitly as such, although it is also a result of wave orbital motion, at least through the wave-induced drift. Some parameterisations for turbulent mixing due to wave orbital motion may also implicitly include the effects of Langmuir circulation even though this is not their aim.

The subject of this review is turbulence generated by the orbital motion of surface gravity waves, and sometimes in the literature this is referred to as "non-breaking wave induced turbulence", or turbulence due to swell. These terms do not preclude that surface waves which do break, or are not in any case "swell", can still generate turbulence through orbital motion as well. Breaking waves may therefore produce turbulence in two ways: by breaking, and by their orbital motion. We are only concerned with the latter process in this paper, but the reader should not forget that in the real ocean both processes must be present. In many cases, from a modelling point of view, it may be that long, non-breaking swell is of more interest since wave breaking from shorter waves is already parameterised in many models, and turbulence due to wave orbital motion may be less important in the vicinity of wave breaking.

We use the terms "turbulent viscosity" and "eddy viscosity" interchangeably, but in keeping with convention, we make a distinction between these, intended to describe the diffusion of momentum throughout a fluid, and "diffusivity", which is usually applied to scalars such as temperature and salinity.

And finally a note on the Stokes drift, or Stokes shear. It is important to distinguish between the wave-induced drift calculated from the irrotational Stokes solution for surface gravity waves, and that found from a model incorporating viscosity. The differences can be substantial in shallow water [Longuet-Higgins, 1953, Kinsman, 1965] and especially when the flow interacts with another shear flow [Phillips et al., 2010, in which may also be found a useful discussion on the terminology]. Here, when we refer to Stokes drift we paper over these differences since that is what is done in most of the studies we discuss in this review, however it should be understood to be an estimation of the wave-induced drift, and whether or not that is important must be considered on a case-by-case basis. We use the terms "Stokes drift" and "Stokes shear" almost interchangeably in this context, although there is of course a difference if one wishes to be exact, or if one is dealing with their mathematical forms. We leave it to the reader to make the correct choice if necessary.

2 The mixing problem

The ocean is of course not fully mixed but stratified. At the surface, during the day and in summer, the sun and atmosphere warm the ocean's surface and uppermost layers, while also evaporating water, creating a thin layer of warm, saline water. This warm, salty water may then be mixed down, both cooling the surface and warming the subsurface. At night, and in winter, as the atmosphere cools, the ocean surface cools as well. Whenever there is a temperature gradient a radiative and diffusive transfer of heat occurs, and similarly for salinity gradients there is a diffusive transfer of salty water into regions of low salinity. These processes are greatly sped up when parts of the fluid are moved into regions of contrasting temperature and salinity, effectively increasing the surface area of contrasting fluids. We usually think of turbulence as what drives this movement of fluids, and there are several mechanisms which can lead to its generation.

As the water changes temperature and salinity its density changes (this is a non-linear process, and there are several equations of state which have been proposed to describe it). This changes the water's buoyancy and can lead to instabilities where less dense water is found underneath denser water. These instabilities lead to the bodies of water changing place, and, as they readjust their positions, to generate turbulence and to mix. On the other hand, where water is denser below, the ocean is stably stratified and turbulence is suppressed, reducing its ability to mix and leaving the ocean stratified. Meanwhile, currents are generated at the surface by the winds, which in turn create shear layers as the water beneath is pulled by viscous forces of the moving surface water and the (relatively) stationary water below. These shear layers, when moving quickly enough, can generate turbulence as well.

Wherever there is a density gradient there is the possibility to have internal interfacial waves. These propagate along regions of strong density gradients called pycnoclines, which usually correspond to regions of strong temperature or salinity gradients, known respectively as thermoclines and haloclines. These internal waves can break, generating turbulence. Tides can generate these waves, especially on continental slopes, and they can also be generated by wind. Though individual waves cannot be predicted with sufficient accuracy to calculate their effect on mixing, several mixing models have been enhanced by internal wave parameterisations. (See the short and useful summary by St. Laurent et al. [2012] for more on these waves.)

At the surface, the wind, while generating currents by imparting a tangential viscous stress on the ocean's surface, also imparts a normal stress, which generates surface gravity waves. Indeed, most of the energy from the wind (except in exceedingly light winds) goes into normal stresses, so most of the wind energy is generating waves, not currents [see for example Kudryatsev and Makin, 2001]. As the waves grow and become steeper they eventually break, both from the action of strong winds and from inherent instabilities within the propagating waves. The breaking dissipates the wave's energy by producing turbulence at the near-surface, which contributes to mixing. As with internal waves, predicting individual breaking events on a grand scale is impossible, so parameterisations aim to represent the effect in the mean.

The effect of all this mixing is to create, near the dynamic surface, a well-mixed upper layer which sits above the relatively static ocean interior. Between the upper layer and the interior is a region of strong gradients of salinity and temperature—respectively the halocline and thermocline—which may coincide but do not always. The region from the thermo-halocline to the surface is known as the mixed layer, though its precise definition varies depending on exactly where you decide to measure from, and what method you use to do so. Some authors also distinguish a “mixing” layer, being distinct from the mixed layer; in this case the mixed layer is the layer of water at more-or-less constant temperature or salinity, and the mixing layer is the region undergoing active mixing by turbulence, which may extend to a greater or lesser depth than the already mixed layer. Much deeper is another region of strong mixing where bottom currents interact with the ocean floor. In coastal areas this is of course important, but in deeper water even if this region is well mixed it will have no immediate impact on the near-surface waters we are presently concerned with.

The affect of biology must also be mentioned. This is harder to quantify, though some work has been attempted on the subject. Needless to say, it depends on the existence of large groups of animals or plants to have much effect on mixing, but according to a recent estimate the mixing from swimming animals of all sizes could be of the same order of magnitude as that generated by wind and tides [Katija and Dabiri, 2009]. Algal blooms can modify surface flow properties for a more indirect impact on mixing, and in shallower waters bottom vegetation and reefs will certainly influence mixing.

With the exception of biology, most geophysical mixing models take into account all of these mechanisms either explicitly in the physics routines or implicitly by parameterising their effects in bulk models. Some of these are resolved to greater or lesser degrees of precision than others, reflecting differences in both our knowledge of the various phenomena and our ability to predict them. Yet there is evidently something missing, since it is widely reported that ocean models underpredict mixing. It is fair to ask whether or not this missing source of mixing is purely a result of our models being inadequately verified as they are or whether indeed there is a mechanism missing altogether. This is not easy to answer, however there is mounting evidence that more mixing can be produced where it is needed in the models by taking into account the surface waves that do *not* break, which of course is the subject of this review.

In parallel with the mixing problem, ocean surface wave modellers have typically dealt with the dissipation of non-breaking waves using an ad hoc formula whereby non-breaking waves dissipate in the same way as breaking waves, only extrapolated to their lower steepness. There is no experimental or theoretical evidence for this, but it was necessary to add to the models in order to model the long swell propagating from distant storms, which can easily traverse ocean basins with very little dissipation of energy. Yet dissipate they do, and extending the breaking formula provided some guidance where there was no theoretical understanding of the process. There are two likely candidates for this dissipation, being wind friction (a kind of inverse of the normal stresses which generate waves in the first place, but it is not an equal and opposite effect) and generation of oceanic turbulence. To some extent both process must occur, but we feel that the evidence points toward oceanic turbulence as being the pricipal mechanism. This leaves us with questions about the nature of this turbulence, questions which are still very much open. There is already a substantial body of literature in which Langmuir circulation has been used to explain the missing source of mixing, and to be sure Langmuir circulation is widespread and has been observed directly. But its impact on mixing is not entirely understood, and attempts to parameterise wave-induced mixing using a Langmuir approach suffer some shortcomings (as, it has to be said, all other wave-related mechanisms do). It is our view that the two mechanisms—if indeed they are really all that separate—must ideally both be represented by models, however we are here concerned with reviewing the work done taking an approach where the wave orbitals themselves are assumed directly responsible for generating the turbulence with or without wind stress. Thus we do not discuss the Langmuir circulation work except in a few cases to make what we feel are meaningful comparisons. For more on mixing related to Langmuir circulation we direct the reader to the numerous fine studies on the subject, including the review by D'Asaro [2014].

3 Oceanic turbulent mixing models

Without providing an exhaustive list, it may be useful here to briefly cover the various kinds of mixing schemes commonly used in oceanographic models. We identify three broad categories:

1. Well-mixed boundary layer bulk models
2. K-profile models
3. Models which attempt to model the turbulence based on transport equations for the physical processes.

The first of these corresponds to a simplified view of the oceanic mixed layer as a layer where all properties, such as salinity and temperature, are unchanged throughout the layer. In this model for the mixed layer the depth of the layer is determined and everything above is effectively mixed instantaneously—as discussed by Large et al. [1994], this unphysical infinite mixing is an undesirable property, though its simplicity lends itself to simple climate models.

The K-profile models, rather than define a mixed-layer depth, instead parameterise the eddy viscosity (denoted sometimes as K or alternatively ν_T). The most popular in oceanographic applications is that of Large et al. [1994], known as the K-Profile Parameterisation (KPP), which was modified for the ocean from the atmospheric mixing model of Troen and Mahrt [1986]. Where it differs most substantially from other K-profile parameterisations is its inclusion of non-local contributions to the mixing—this means that aside from local properties of the fluid, the mixing at any point is influenced by fluxes at the edge of the boundary layer (that is the layer under the influence of surface forcing) and eddies whose maximum size is determined by the depth of the layer. In these models, whether local or non-local, properties such as the wind stress, shear, and Richardson numbers are used to determined the shape of the eddy viscosity profile with depth. This can then be used to determine the amount of mixing in the oceanic transport equations for momentum and scalars through parameterisation of the turbulent fluxes,

$$\overline{u'w'} = -\nu_m \frac{\partial u}{\partial z}, \quad \overline{C'w'} = -\nu_C \frac{\partial C}{\partial z}. \tag{3.1}$$

Here u is the horizontal velocity, w the vertical velocity, and C a scalar (such as temperature or salinity). The velocities may be decomposed into

$$u = U + u', w = W + w' \tag{3.2}$$

where U and W are the mean horizontal and vertical velocities, and the primed variables are the turbulent deviations from the mean. ν_m and ν_C are the eddy viscosities for momentum and scalars respectively (the same as K in the K-profile models; note that ν_m and ν_C are frequently treated as the same, although in fact even for different scalars the diffusivities are different). There are both advantages and limitations to using these models: in their favour, they are usually quick to compute and do not require complete knowledge of the parameters in order to generate a realistic mixed layer, and in many situations they out-perform more physical models. On the other hand, because they do not attempt to solve the transport equations for turbulent kinetic energy they can miss some of the dynamics. They also require some extra work if an extra source of turbulent mixing is to be added, since sources of mixing are not additive in terms of eddy viscosity. This fact, we will show, becomes important later when we consider how to include a wave-induced effect.

The final type of model we will consider is one where the physics of the turbulence is resolved. Most geophysical turbulence models of this type are from a class of models known as two-equation models. The first equation is the transport equation for turbulent kinetic energy (TKE), and is derived from Reynolds averaging the equations of motion for a fluid. It usually takes the form

$$\frac{\partial k}{\partial t} + u_i \frac{\partial k}{\partial x_i} = D + P + B - \epsilon \tag{3.3}$$

where k is the turbulent kinetic energy, u_i and x_i are the velocity and coordinate vectors written using the Einstein summation convention. D is the diffusion term (i.e. it represents the diffusion of TKE itself), P is the production of TKE by mean shear, B is the production of TKE by buoyancy, and ϵ is the dissipation of TKE. Note that these production and dissipation terms are additive, unlike eddy viscosity.

The dissipation ϵ may be related to the TKE and the integral length scale (scale of the large, energy-containing eddies) by dimensional arguments, so we may write

$$\epsilon \sim \frac{k^{3/2}}{l}. \tag{3.4}$$

Notwithstanding a constant of proportionality, the problem of determining the dissipation is then equivalent to that of determining the integral length scale. So-called one-equation models impose a diagnostic equation to determine one of these variables, but since they vary with the flow it makes sense to try to model this explicitly; a second transport equation may be formulated:

$$\frac{\partial \psi}{\partial t} + u_i \frac{\partial \psi}{\partial x_i} = D_\psi + \frac{\psi}{k} \left(c_1 P + c_2 B - c_3 \epsilon \right). \tag{3.5}$$

In writing this equation we have followed Umlauf and Burchard [2003] in using the generic variable ψ. The choice between using dissipation or length scale, or indeed any other variable or combination of variables which can be related to the dissipation, is notionally equivalent. So while details differ between, say, a k-ϵ or k-kl model, the physical processes they are representing are the same, and can be related back to the generic equation. (Although we note that their behaviour is not always the same. In fact, the purpose of the generic model using ψ was to compare them—see Umlauf and Burchard [2003].) The variable ψ is therefore a proxy for dissipation, and we can see that this equation is similar to the TKE equation. But unlike the TKE equation, this one has little basis in theory, but instead is simply modelled off the transport equation for k. Nevertheless, it has been found, depending on the implementation, to describe observed flows quite well [Wilcox, 1998]. In geophysical applications, one of the most popular implementations is the level 2.5 Mellor–Yamada model, which is a k-kl model. It was originally proposed by Mellor and Yamada [1982] but has since been modified by several authors in order to better represent their observations and, in some cases, to include other physical processes. While it has no obvious advantages over other two-equation models, because of its widespread use it is worthy of special mention, and we will see how it has been used in research involving wave-induced mixing.

Depending on the application, one or other of these models may be more suitable. Coarser climate models, for example, probably would not benefit from some of the fine structure generated by a mixing model based on transport equations for the turbulence, and a bulk model may work just as well; a high resolution model would probably benefit from that detail. Also to be considered are numerical issues which may occur when using one of these models at resolutions not anticipated by the ocean model developers. Perhaps less obviously, in some cases a bulk model may outperform a physics based transport model, especially when elements of the physics are missing or unknown. In this case, a model which does not explicitly model the physical processes, but instead tries to reproduce observed mixed layer profiles in the mean, may be advantageous.

4 Historical development

4.1 Early publications

Until quite recently, oceanographic models have not included the effect of wave-induced mixing, except that from wave breaking, yet the idea goes back at least as far as the early 20th Century. Jeffreys [1920] almost took it as a given that waves produced oceanic turbulence:

> If turbulence can be largely attributed to wave motion, the way it dies down at great depths is readily accounted for; for wave motion diminishes as tho depth increases, and at a depth equal to the wave length it has practically ceased. This suggestion is confirmed by the fact that the depth where turbulence shows marked diminution is actually of the same order of magnitude as the length of Atlantic waves.

The reference to "wave motion" and its diminution to almost nothing at the depth of the wave length indicates that he is referring to wave orbital motion, and not wave breaking, whose turbulence scales with the wave height.

There was little in the way of a physical explanation to motivate Jeffreys' assumption. In hindsight it seems to have rested on the rather mundane observation that if there is any shear, which there is in an otherwise stationary fluid underneath a surface wave, then there will be some capacity to generate or interact with turbulence. Dobroklonskiy [1947], inspired by Jeffreys' attempt, sought a more rigorous explanation, atypically using trochoidal, or Gerstner waves. Normally the mathematical simplification for surface waves is the sinusoidal Airy wave, which is taken in the limit of infinitesimally small wave height and which is irrotational. The Stokes wave is an expansion of this, which enables finite-height solutions but which is still irrotational. An alternative approach is the Gerstner wave, which eschews the finite-height assumption but enforces circular orbits. The result is a wave which is rotational and of finite height, whose surface traces a trochoid rather than a sinusoid, and which in the limit reduces to an Airy wave. Using these, Dobroklonskiy derived a formula to estimate the eddy viscosity under waves based on Prandtl's mixing length hypothesis,

$$\nu_m = \frac{\pi \rho_w r^2}{18} \frac{H^2}{T} e^{2\kappa z} \left(1 - \frac{H^2 \kappa^2}{4} e^{2\kappa z}\right)^3, \tag{4.1}$$

where H is the wave height, T is the period and κ the wave number. The constant r, related to the mixing length, was set to be between 0.36 and 0.40 from experiments in pipes, which needless to say may not be appropriate here. The formula gave an estimate to within an order of magnitude of the data available at the time.

One early opinion on the role of turbulence on waves was that of Suthons [1945], who apparently tried to explain wave dissipation through the eddy viscosity. According to Groen and Dorrestein [1950], Suthons' reasoning was curious in that it seems to have implied that waves could get longer merely because the eddy viscosity transferred energy downwards, deepening the effect of the wave motion. Nowadays we would think that it should be the other way around, and that longer waves should be able to affect eddy viscosity at greater depths than shorter waves. Groen and Dorrestein evidently felt the same way and presented an alternative hypothesis based on an equation introduced by von Weizsäcker [1948] and Richardson and Stommel [1948], whereby the eddy viscosity was related to the wave length as

$$\mu(\lambda) = m\lambda^{4/3} \tag{4.2}$$

where m is a constant of proportionality, μ is the dynamic viscosity and λ is the wave length. Groen and Dorrestein interpreted their results as demonstrating that short waves could be attenuated more quickly by eddy viscosity, which served to lengthen the swell; this was intended to supersede a wind friction mechanism proposed by Sverdrup [1947].

4.2 Similarity arguments and first serious theoretical treatment

Bowden [1950] questioned both Groen and Dorrestein's assumption that their formula would apply in the case of ocean surface waves, and whether the correct length scale to use in this case should be wave length and not wave height instead. (This question would become a recurring theme.) Bowden considered a wave as being defined by its wave length, period and amplitude, and on assuming the simplest power law involving these quantities derived the expression for eddy viscosity due to waves

$$\nu_w \sim a\sigma\kappa^{-1}, \tag{4.3}$$

where a is the wave amplitude, σ is the angular frequency, the deep water dispersion relation has been applied and the constant of proportionality is assumed to vary slowly enough to be regarded as constant. Later authors derived entirely different expressions using these same three parameters (see section 5.5.3).

The formula for the mean dissipation of wave energy due to molecular viscosity may be given by [Lamb, 1932, article 348]

$$D = 2\mu\kappa^3 c^2 a^2 \tag{4.4}$$

where c is the phase speed of the wave and μ is the dynamic viscosity of the fluid. By substituting his expression for eddy viscosity into this equation Bowden presented an equation for the rate of wave dissipation per unit area by eddy viscosity, which we write, with the constants being absorbed into the constant of proportionality C_1, as

$$D_T = C_1\kappa^3 c^3 a^3. \tag{4.5}$$

He then applied von Kármán's similarity hypothesis [von Kármán, 1930] for shear flows to the two-dimensional flow of wave orbitals, and obtained a formula which agreed with (4.5). Since the formula was depth-integrated, he also presented one showing the mean rate of loss of wave energy per unit volume at depth z,

$$dD_T = C_1\kappa\sigma^3 a^3 e^{3\kappa z}. \tag{4.6}$$

The integral over all depths leads to equation (4.5).

Bowden's study was, as its title indicates, concerned with the dissipation of ocean waves due to turbulence. However it is clear that a diminution of wave energy by turbulence must also result in an augmentation of turbulent energy. We will revisit Bowden's analysis in this context later on when we consider some more recent experimental work. Meanwhile, an almost passing comment in a technical report by Francis et al. [1953] offers a tantalising, though highly speculative, possibility:

> A point of some interest lies in the high stresses observed quite near the surface. It is clear that the stress at the very surface must be zero on this windless day; yet at only 20 cm below it was as high as at all other points through the fluid. Either the instrument must in some subtle way give a false reading, possibly due to its large size compared with its submergence, or some hitherto unsuspected complication is caused by the free surface.

Could this in fact be the first recorded observation of turbulence generated or otherwise modified by non-breaking surface waves? It is, unfortunately, unclear what it was they observed based on the scant information provided, and indeed whether waves of sufficient size were present in the very calm weather conditions. (Further on they describe situations where movement due to wind-generated waves compromised the ship-mounted instrument's measurements, but it is nevertheless possible that waves of a large enough dimension were present at this time—no measurements of waves were presented by the authors.)

Nowadays potential wave theory is commonly used to solve a wide array of problems, and spectral wave models of the kind used to forecast ocean waves assume its validity. But as Longuet-Higgins [1953] demonstrated, the inclusion of viscosity in the equations of motion can for some problems radically alter the resulting calculations. It cannot be taken as a given, therefore, that potential theory will always give useful results. Phillips [1961] enquired as to whether turbulence could appreciably alter the results of potential wave theory with regard to ocean swell. His conclusion, based on order of magnitude estimates for the dynamics presumed relevant to a wave–turbulence system, was that the turbulence maintained by the wave motion was not enough to alter the dynamical predictions of potential theory. That this is at least partially true is self-evident: potential theory has been remarkably successful at modelling water waves. According to Phillips' analysis, the time taken for a wave to reach $1/\sqrt{2}$ of its initial height is

$$\vartheta_a = \frac{\mathrm{Re}_w}{2\pi\kappa^2 a_0^2} \tag{4.7}$$

where a_0 is the initial amplitude of the waves, and a wave Reynolds number is defined as

$$\mathrm{Re}_w = \frac{\sigma}{\nu\kappa^2}, \tag{4.8}$$

with ν the kinematic molecular viscosity. Using this formula, we may calculate that a 15 second wave of height 5 metres would take more than 25 billion periods to dissipate that amount, an immense amount of time corresponding to a distance of around 4 billion kilometres, or more than 26 times the distance to the sun. Measurements suggest a similar attenuation occurring after only several hundred kilometres [Young et al., 2013], and while this could be caused by other mechanisms, it is also possible that important pieces are missing from Phillips' analysis. (It's worth mentioning that just by changing the way the Reynolds number is calculated, for example using an amplitude-based method such as equation (4.11), the number ceases to look so ridiculously oversized.) In his description of Phillips' work, Kinsman [1965] is careful not to put too much trust in the result, and perhaps it ought not be surprising if we find that the analysis is incomplete. Turbulence from other sources is missing, precluding the possibility that the interaction of strong turbulence and waves might lead to greater attenuation, and many suppositions are made along the way.

4.3 A unique approach from China

Around the same time as Phillips's work, two authors from China during the early 60s, Cao [1962] and Ma [1965], sought to address a problem they found with some earlier parameterisations where the vertical motion of the particle orbits was averaged out. The prevalence of the problem seems to have been somewhat exaggerated—Bowden [1950], for example, and Dobroklonskiy [1947], whose approach they appear to have been inspired by, especially in the use of Gerstner waves, did not make this assumption. However it would, as we shall see, surface in later work by other authors.

Cao [1962] and Ma [1965] determined the mixing length by combining two independent equations: one according to Prandtl's mixing length hypothesis, and the other following Taylor. By eliminating the mixing length they were able to form equations for the turbulent fluctuations u' and v', and therefore also the Reynolds stress $\tau = -\rho_w \overline{u'v'}$. This enabled the next step, which was to estimate the turbulent dissipation from the Reynolds-averaged turbulent kinetic energy equation, equation (3.3), where the production of turbulence, assumed to be in balance with the dissipation, is given as

$$P = \tau_{ij} \frac{\partial U_i}{\partial x_j}. \tag{4.9}$$

Following Ma, this lead to an expression for the dissipation in terms of a non-dimensional unknown x,

$$\epsilon \approx 0.84 x^8 \rho_w a^4 \kappa \sigma^3. \tag{4.10}$$

Though the details are not presented, Ma calculated x by assuming that all of the wind energy input into the waves would be completely dissipated by the oceanic turbulence. The value determined, $x = 0.48$, is thus probably a little too high. Substituting it back into the dissipation equation, the constant becomes 0.002367, which is not too much higher than the constant in the much later derived dissipation equation (5.37).

Cao approached the problem in a similar way but for the dissipation formula additionally used equation (4.4), the same as Bowden [1950], and parameterised turbulent viscosity in terms of wind speed, wave age and wave steepness. The result was compared with dissipation determined directly from the Reynolds-averaged dissipation rate (4.9), and some of the parameters fixed, but an unknown remained.

Another important result from Ma's work is the definition of Reynolds number,

$$\mathrm{Re}_w = \frac{u_{\mathrm{orb}} 2a}{\nu}. \tag{4.11}$$

Though it was not used in the analysis leading to the dissipation equation it is interesting to compare it with Phillips's [1961] definition, which features wave length as the length scale instead of, as here, wave amplitude. Ma also performed experiments for which few details are given except that the critical Reynolds number fell between 2000 and 14000.

At the time these papers were written Gerstner waves had never been observed in the laboratory [Kinsman, 1965]. More recent work suggests that Gerstner waves can in some circumstances and in some ways outperform Stokes waves at modelling observed wave properties in the lab [see for example Monismith et al., 2007], but it remains a stretch to use them to model ocean waves more generally if for no other reason than the orbits are closed.

4.4 Direct observations and first laboratory experiments in the west

Phillips' analysis might suggest that any interaction between waves and turbulence would be so small as to have no effect on ocean wave prediction or on oceanic turbulence. Not long after, preliminary results from an observational study by Shonting [1964], followed a few years later by a more complete study also by Shonting [1970], indicated the opposite. What Shonting measured was a downward flux of momentum greater than would be expected without the presence of waves. While this does not necessarily mean the same thing as producing turbulence, it does allow for a transport of turbulence into regions it might not otherwise reach, potentially leading to a deeper mixing layer. The effect measured by Shonting occurred in a wind sea, where the wind was still actively imparting energy to the waves.

In a pair of papers, Yefimov and Khristoforov [1971a, 1971b] reported on field observations they made in the Black Sea of wave spectra and turbulence in the water. They showed that the correlation between the surface wave elevation spectrum and the underwater velocity spectrum broke down with depth, sooner for higher frequency waves. This is to be expected, since because of the exponential decay of the wave orbitals the high frequency wave motion can not reach further down, and what is left (assuming the absence of currents and other low frequency waves) is turbulence. Near the surface, where the correlation between high frequency wave elevation and water velocity was very low, they determined that the turbulence was characteristic of being generated by waves, differing in several ways from that usually observed in flow across a wall [1971a]. Moreover they reported turbulence as being significantly higher under more energetic waves, underscoring the connection between turbulence and waves. Their study appears to be the first where the authors claim to have made an unequivocal field observation of turbulence generated by wave orbital motion.

Yefimov and Khristoforov [1971a] presented their observational data along with several quantitative estimates. Particularly interesting was that for a non-dimensional "transition frequency", Ω_t. To get this they first defined a dimensional transition frequency σ_t, which corresponds to the frequency for a given depth at which the correlation function $R_{\eta w^2}(\sigma, z) = 0.25$. This function measures the correlation between the surface elevation η and the vertical velocity, indicating whether the measured velocities are of the waves or of turbulence. It is calculated as

$$R_{\eta w^2}(\sigma, z) = \left(1 + \frac{S_t(\sigma, z)}{S_{ww}(\sigma, z)}\right)^{-1}, \tag{4.12}$$

where $S_t(\sigma, z)$ is the turbulence velocity spectrum (assuming isotropy, otherwise the vertical turbulence velocity is more appropriate) and $S_{ww}(\sigma, z)$ is the vertical component of the wave orbital velocity. Two dimensionless parameters are defined:

$$\beta_1 = \sigma_t \sqrt{\frac{z}{g}} \tag{4.13}$$

and

$$\beta_2 = \sigma_p \sqrt{\frac{\eta_{\rm rms}}{g}}, \tag{4.14}$$

where σ_p is the peak frequency and $\eta_{\rm rms}$ is the root mean square surface elevation, used to defined a characteristic vertical scale for the waves. Ω_t is then simply β_1/β_2, and their data

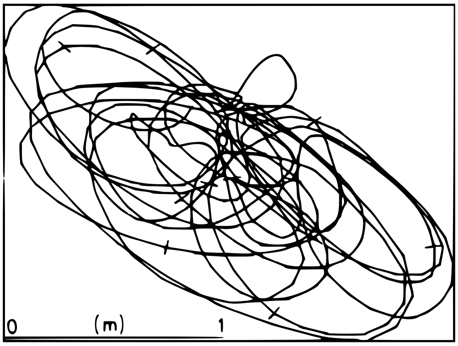

Fig. 4.1. Water particle motion under growing waves recorded during a field campaign reported by Cavaleri and Zecchetto [1987]. The record shows oblique orbits caused by the horizontal and vertical velocities being out of quadrature, leading to a Reynolds stress. [Figure after Cavaleri and Zecchetto, 1987]

suggests that it is constant, with a mean value of 8.3, although there is of course scatter which they attribute to other sources of turbulence such as mean shear, and the approximation for β_1 not being appropriate for developing seas.

It seems to be about this time that researchers began to investigate the interactions of surface waves with turbulence in the laboratory, the first two efforts appearing in the same year: the thesis by Skoda [1972] and the paper by Green et al. [1972]. The latter of these examined waves in the capillary regime as well as gravity waves, and they noted that their longer waves (over 2 Hz) were long enough to interact with the submerged turbulence-generating grid. In both studies waves propagated over turbulent water and it was found that the waves were attenuated by the presence of turbulence. Green et al. [1972] even determined that the wave attenuation was due mostly to dissipation, as opposed to scattering of waves, a phenomenon discussed by Phillips [1959]. Green and Kang [1976] performed experiments using convective turbulence instead of grid turbulence, also observing wave attenuation.

Meanwhile, seemingly unaware of this experimental work, oceanographers continued to make measurements which could not be explained adequately by the prevailing theory. Cavaleri and Zecchetto [1987] discussed some of these studies, including one where the measurements and theory were apparently found to be in agreement [Battjes and van Heteren, 1983]. But most interesting were their own results, based on data spanning back several years prior. In these they found, just as had Shonting [1970], that the horizontal and vertical velocities of the wave orbitals were out of quadrature in a variety of different wave regimes, but especially for actively generated wind waves, and effectively not at all for swell. Some examples of the orbitals are shown in figure 4.1. It would take over two decades for a theoretical explanation of their observations to appear in a paper by Nielsen et al. [2011]. The theory shows that growing or decaying waves produce orbital velocities out of quadrature, generating Reynolds stresses. It follows that for long swell, which decays only very slowly, this mechanism must be weak, possibly insignificantly so.

4.5 Applying wave-induced turbulent mixing to a numerical ocean prediction model

With the underlying aim of trying to improve weather forecasting models, Jacobs [1978a] developed a model for wave-induced turbulence. This constitutes what we think may be the earliest attempt at a practically applicable parameterisation in a numerical modelling context. It is a relatively straightforward approach based on a calculation of the gradient of the mean orbital speed of the waves and adding it to the vertical shear term in several different bulk formulas for eddy viscosity. A wave-based gradient Richardson number is defined as

$$\mathrm{Ri}_w = -\frac{g}{\rho}\frac{\partial \rho}{\partial z}\left(\left|\frac{\partial \mathbf{V}}{\partial z}\right| + \left|\frac{d\overline{U_{\mathrm{orb}}}}{dz}\right|\right)^{-2}, \tag{4.15}$$

where $\mathbf{V}(z)$ is the mean horizontal velocity vector and $\overline{U_{\mathrm{orb}}}(z)$ is the mean of the wave orbital velocity at a given depth z. For stable conditions (defined as $\mathrm{Ri}_w \geq 0$) the eddy viscosity for momentum is expressed as

$$K_m = k_1^2 (z + \delta\lambda/2)^2 \left(\left|\frac{\partial \mathbf{V}}{\partial z}\right| + \left|\frac{d\overline{U_{\mathrm{orb}}}}{dz}\right|\right)\sqrt{1 + 10\mathrm{Ri}_w} \tag{4.16}$$

with similarly formed equations for different Richardson numbers and for scalars (conductivity-diffusivity). Here k_1 is the Kitaigorodskii constant, δ is the steepness and λ is the wavelength. Interestingly, when compared with the equations Jacobs presented where waves are ignored, the waves are included in two places: as an additional velocity shear (treated as equivalent to the usual shear due to mean velocity) and as an extra factor in the length scale (an amplitude dependence, $\delta\lambda/2$). This means that the mean shear due to currents also gets augmented by a wave-related parameter.

Using data from the Barbados Oceanographic and Meteorological Experiment (BOMEX, Jacobs [1978b]) he found that the eddy viscosity parameterisations were generally well served by including the wave effect. We are unaware of any oceanographic or atmospheric prediction models in operational environments which use any of Jacobs' parameterisations, however it is worth noting that he estimated wave length by parameterising it with wind speed, assuming a fully developed sea via the steepness parameter δ, but his equations could easily be applied to a set of predefined wave dimensions calculated independently of the wind, and could therefore be a useful tool for modellers to test.

4.6 Modern theoretical work and experiments

In a pair of papers, Kitaigorodskii and Lumley [1983] and Kitaigorodskii et al. [1983] examined turbulence in the presence of surface gravity waves. Their work spanned analysis and observation, and they sought to apply the theory to the observed characteristics of the boundary layer which could not be explained by the usual boundary layer scalings where waves are ignored. An important aspect of their work was to separate the motion into three components, rather than the usual two. Normally turbulence is characterised by dividing the motion into a mean part and a fluctuating part, as in equation (3.2), so that the quantities may be expressed as

$$x = X + x' \tag{4.17}$$

where x stands for a component of a vector quantity or a scalar, X is the mean value and x' is the fluctuating part, understood to represent the turbulence. For a shear flow with mean velocity U, and for which the turbulent fluctuations u' disappear when Reynolds averaged (in other words $\overline{u} = U$), this is a reasonable description of the motion. By Reynolds averaging the Navier–Stokes equations a correlation results where the fluctuating terms, the x', remain—this is the Reynolds stress, expressed in Einsteinian notation as

$$\tau_{ij} = -\rho\overline{u_i'u_j'}, \tag{4.18}$$

where ρ is the density of the fluid. The presence of waves complicates the story somewhat. One way of dealing with them would be to include the waves with the mean motion. This makes sense on one level: the waves are, at least in an idealised sense, periodic, thus they are fundamentally different to the stochastic turbulence. Under this assumption, when Reynolds averaging the equations of motion there is no correlation between the waves and the turbulence. However it seems improper to think of the waves in this way—true, they cannot be considered turbulent motions, but they are also distinct from the mean motion, which in this model for fluid motion never changes (more strictly, it changes slowly compared with the turbulence). The three-way separation acknowledges this explicitly:

$$x = X + x^w + x' \tag{4.19}$$

where x^w is the component of the variable due to the wave motion. Now a bunch of extra correlations are produced. Anis and Moum [1995] describe these correlations and also attempted to relate them to observational data, focussing on two mechanisms in particular. One of these, the vertical transport of TKE by waves, could be derived assuming irrotational wave motion,

$$-\frac{\partial\overline{w^w\frac{1}{2}u_i'u_i'}}{\partial z}, \tag{4.20}$$

where w is the vertical velocity and w^w is the wave component of the vertical velocity. They explained this as follows: when the vertical velocity is upward the turbulence near the surface cannot move beyond the surface, therefore it can only diffuse horizontally and downward. When the wave orbital is on its downward cycle it brings a patch of turbulence with it, which diffuses further down, before that patch is brought up again on the next cycle. This argument does not sound quite satisfying, however, since irrotational wave orbital motion does not move particles to and from the surface.

The other mechanism they examined required rotational motion:

$$-\overline{u_i'u_j'\frac{\partial u_i^w}{\partial x_j}}. \tag{4.21}$$

Note that u_i^w and x_j can refer to any of the three directional components, so this is a general expression for turbulence production by the shearing motion of the waves, in contrast to, say, just the Stokes drift. Anis and Moum [1995] attempted to relate these mechanisms to their observations, complicated as they were by the presence of breaking waves.

In order to completely avoid the issue of waves interacting with the side wall of a laboratory tank, Ölmez and Milgram [1992] performed experiments where the waves propagated radially from a central wave maker. They measured the dissipation of the waves before they reached the edge of the tank, taking into account the apparent dissipation of the waves as their energy was spread over an increasingly long circumference. By propagating these waves over turbulence generated by an oscillating grid they found that the dissipation of the waves was enhanced by turbulence. A key finding was that in the regime of small steepness to which their experiments were limited they found no dependence on wave amplitude. They distinguished between two mechanisms which could lead to wave decay: dissipation of waves by vertical mixing by turbulence, and transfer of energy from waves to turbulence (presumably by stretching vortex lines). In part because of the independence on wave amplitude they favoured the former. The waves they generated were very small, with wavelengths between 6 and 10 cm and amplitudes of a few millimetres, so specific results might not be immediately applicable to larger waves in the ocean. They did find that the data of Skoda [1972], who generated waves of slightly longer wave lengths in a flume, were in rough agreement. Further experiments by Milgram [1998] were designed to examine the damping of waves in the presence of both turbulence and a surfactant. This time the waves were rectilinear waves in a flume, and although the turbulence and surfactant effects were found to be additive, the greater interest for us lies in the fact that the turbulence served to dissipate the waves. Again the waves were short, in the gravity–capillary regime.

Benilov et al. [1993] and Benilov [2012] showed that vorticity grows under the passage of linear surface waves, excepting the component directed along the crests. (The analysis is presented in both sources cited but is more readily available in the latter one.) For z positive upwards, the velocity potential for linear waves is of the form

$$\phi = -\frac{ag}{\sigma}\cos\theta e^{\kappa z} \tag{4.22}$$

where $\theta = kx - \sigma t$ and we assume that the waves are directed in the x direction. The velocities are then

$$u(x, z, t) = \frac{a\kappa g}{\sigma}\cos(\theta)e^{\kappa z} \tag{4.23}$$

$$w(x, z, t) = -\frac{a\kappa g}{\sigma}\sin(\theta)e^{\kappa z}. \tag{4.24}$$

A small perturbation $\tilde{\boldsymbol{u}}$ is applied to u and w, such that

$$|\mathbf{u}| \gg |\tilde{\mathbf{u}}| \quad \text{and} \quad \left|\frac{\partial u_i}{\partial x_j} + \frac{\partial u_j}{\partial x_i}\right| \gg \left|\frac{\partial \tilde{u}_i}{\partial x_j} + \frac{\partial \tilde{u}_j}{\partial x_i}\right|. \tag{4.25}$$

In other words the vorticity field is negligible from the point of view of the wave motion. The vorticity equation may then be expressed simply as

$$\frac{d\boldsymbol{\omega}}{dt} = (\boldsymbol{\omega}\cdot\nabla)\mathbf{u}. \tag{4.26}$$

The fluid particle motions about their equilibrium point, $\boldsymbol{\xi} = \boldsymbol{x} - \boldsymbol{x_0}$, may be described by the formulas

$$\xi = x - x_0 = a\cos\theta_0 e^{\kappa z_0} \tag{4.27}$$

$$\zeta = z - z_0 = a\sin\theta_0 e^{\kappa z_0} \tag{4.28}$$

$$\theta_0 = \kappa x_0 - \sigma t, \tag{4.29}$$

giving formulas for $\mathbf{x} = \boldsymbol{\xi} + \mathbf{x_0}$. Using these together with the velocities (4.24), the right hand side of the vorticity equation may be written as

$$\sigma a \kappa e^{\kappa(\zeta+z_0)} \Bigg\{ \widehat{\boldsymbol{x}} \Bigg[\omega_x \cos(\kappa[\xi + x_0] - \sigma t) + \omega_z \sin(\kappa[\xi + x_0] - \sigma t) \Bigg] \\ + \widehat{\boldsymbol{z}} \Bigg[\omega_x \sin(\kappa[\xi + x_0] - \sigma t) - \omega_z \cos(\kappa[\xi + x_0] - \sigma t) \Bigg] \Bigg\}. \quad (4.30)$$

If the displacements are small (i.e. ξ and ζ are small) then power series expansions lead to, at second order,

$$\begin{aligned} \frac{D\omega_x}{Dt} &= \sigma a \kappa e^{\kappa z_0} \Bigg[\omega_x \cos\theta_0 + \omega_z (\sin\theta_0 + a e^{\kappa z_0}) \Bigg] \\ \frac{D\omega_y}{Dt} &= 0 \\ \frac{D\omega_z}{Dt} &= \sigma a \kappa e^{\kappa z_0} \Bigg[\omega_x (\sin\theta_0 + a e^{\kappa z_0}) - \omega_z \cos\theta_0 \Bigg]. \end{aligned} \quad (4.31)$$

Thus the vorticity may be modified by the wave motion, excepting the component in line with the wave crests (angular momentum vector pointing along the crest).

Following this analysis, Benilov et al. showed numerically that the nonzero equations in (4.31) are unstable, meaning that if any vorticity unaligned with the wave orbital motion exists it will be amplified by the waves. This gives a clear physical mechanism for transferring energy from waves to turbulence. Though the analysis is only to second order, this is also most likely the mechanism at work in the large eddy simulation results of Babanin and Chalikov [2012] which we will discuss below. An important corollary of Benilov's analytical result is that if the problem domain is two-dimensional then the waves do not interact with the vorticity field. The problem must be approached in three dimensions, even if the waves themselves are treated as infinitely long-crested.

Datla [1996] performed experiments in a long flume with oscillating grids generating turbulence. The waves were much larger than those studied by Ölmez and Milgram [1992], Milgram [1998] and Skoda [1972], typically of period around 1 s, or wave length about 1.6 m assuming the deep water dispersion relation holds—in this case it does since the mean water depth is about 1.65 m. A spectrum of waves with a peak period of about 1.8 seconds, or roughly 5 m, was also run, and here the deep water approximation does not hold. Turbulence was generated with grids some distance away from the wave maker, and most of the time they observed a reduction in wave height, and an increase in turbulence. One problem in this study was that, unlike with some of the others, the waves were run for very long periods of time, some tens of minutes. Reflections were minimised by the use of a beach, but running waves for that length of time in a flume generates a return current in response to the wave-induced drift. Here the shear generated by the return flow was not measured, and instead a vertically integrated transport was calculated. This means that shear-generated turbulence was unaccounted for. Although this might mean that the measurements of turbulence need adjustment, the effect on the wave height clearly demonstrates a reduction of wave energy due to water-side turbulence.

Datla added an interesting innovation to previous studies by observing that the grid generated a mean vertical flow which would lead to surface convergence and divergence zones. This was compensated for by oscillating the grids in an asymmetrical fashion, just enough to eliminate the mean vertical transport, a technique whose absence, they noted, may have some bearing on measurements of some earlier studies.

The rapid distortion model of Teixeira and Belcher [2002] seems to have been intended to study the role of turbulence in forming Langmuir circulations, but in their examination of the interaction of waves and turbulence they went beyond merely considering the Stokes drift. Their work considered turbulence of small length scale distorted by steep enough irrotational gravity waves. They showed that Stokes drift could modify the turbulence field to resemble Langmuir circulation, where instead of a wind-generated shear layer the Stokes drift acts on the vorticity in the turbulence field. They also described how a passing wave could (with the Stokes drift neglected) distort the turbulence symmetrically by stretching and compressing it with the passage of crests and troughs. Teixeira and Belcher also showed formulas for the strain tensor, including non-symmetric components. These terms may be key to reconciling their results with the other theoretical work by Benilov et al. [1993] and Kitaigorodskii and Lumley [1983]. The symmetric compression and decompression of vorticity by the surface oscillations (neglecting Stokes drift for the moment) seems, in light of Benilov et al.'s [1993] work, to leave out a crucial dynamical component.

4.7 Introduction into geophysical numerical models

As geophysical models became more sophisticated more and more physical processes had to be accounted for directly. Where ocean slab models used to be sufficient for climate models, it is now increasingly common to replace them with dynamic ocean models. Similarly, where mixed layers were once parameterised simply as an instantaneously mixed layer near the surface of the ocean, now it is common to attempt to calculate the rate of mixing using sophisticated turbulence closure schemes, necessitating a much more detailed knowledge of oceanic physics, especially within and near the mixed layer. So as attention turned toward these processes it became apparent that the models were frequently incapable of producing the mixing observed, and attempts at filling in the gap led some modellers to consider wave orbital motion as a possible source for this mixing.

Large-scale modelling studies with mixing attributed to wave orbital motion did not take place until the beginning of the new century. (At this time some modellers also began applying the theory of Langmuir circulation to mixing, following the work of McWilliams et al. [1997]. While this is outside the scope of this review some of these concepts are dealt with briefly in section 6. For more we direct the reader to the review on upper-ocean turbulence by D'Asaro [2014] and the review on Langmuir circulation by Thorpe [2004].) A new parameterisation, based on Prandtl's mixing length hypothesis applied to wave orbitals, was introduced by Qiao et al. [2004] and applied to an ocean model with considerable success. A large body of work revolving around applications of this parameterisation in different models and modelled environments now exists, and is examined at length in section 5.1. More interested in sediment suspension, Pleskachevsky et al. [2005] added the effect of waves to their model. This parameterisation was light on theoretical motivation, but a later study by Pleskachevsky et al. [2011] invoked some interesting (though unverified) theoretical arguments. Both of these are examined in section 5.

It is in the context of these modelling studies that the recent experiments by Babanin [2006], Babanin and Haus [2009] and Dai et al. [2010] should be understood. It may be said that they belong to a different experimental tradition than the work hitherto described, less focussed on the fluid dynamical aspects of turbulence and wave interaction and more on the practical application of this knowledge to ocean modelling and wave prediction. The disconnect is such that none of the earlier experiments by Green et al. [1972], Skoda [1972], Ölmez and Milgram [1992], Milgram [1998] or Datla [1996] were cited in the above publications. Needless to say, this has little if any bearing on the results, but it does underscore the relative neglect of the subject in oceanographic circles until recently.

In the first of these experiments, by Babanin [2006], dye was dispersed by waves in a flume. The experiment was designed to test the hypothesis of a wave Reynolds number defined in terms of wave amplitude, in contrast to the one proposed by Phillips [1961], whose length scale was the wave length. It may be expressed as

$$\mathrm{Re}_w = \frac{a^2\sigma}{\nu}, \tag{4.32}$$

which differs by only a factor of two to the definition proposed by Ma [1965], (4.11). Since the amplitude of the wave orbitals decays with depth this may be expressed as

$$\mathrm{Re}_w = \frac{a_0^2 e^{2\kappa z}\sigma}{\nu}. \tag{4.33}$$

If a critical Reynolds number, $\mathrm{Re}_{\mathrm{cr}}$, is defined, a critical depth, z_{cr}, may be determined,

$$z_{\mathrm{cr}} = -\frac{1}{2\kappa}\ln\left(\frac{\mathrm{Re}_{\mathrm{cr}}\nu}{a_0^2\sigma}\right). \tag{4.34}$$

To estimate $\mathrm{Re}_{\mathrm{cr}}$ from these expressions, Babanin used the depth of the bottom of mixed layer in the Black Sea during conditions where turbulent mixing was thought to dominate mixing. The number was in the vicinity of $\mathrm{Re}_{\mathrm{cr}} = 3000$, which is consistent with the rather broader range measured by Ma [1965]. By increasing the amplitude of the waves in the lab experiment, the wave Reynolds number could be controlled. Observation of the dye's dispersal suggested that the number was a good predictor of turbulent motion. Using dye is no longer usually considered to be an accurate way of estimating the existence of turbulence [Jason Monty, private communication], so these experiments cannot be considered to be conclusive. The waves are also quite long, with periods of about 1.5 seconds, so in the tank's water depth of about a metre the wave orbital motion would be felt at the bottom, presumably producing more turbulence, though since the turbulent dispersal of the dye occurred near the surface it seems unlikely that effects from the tank bottom were an important factor. Babanin [2006] also showed that global critical depth estimates for the mixed layer were consistent with mixed layer depth climatology, and following on from this Babanin et al. [2009] used equation (4.34) to estimate mixed layer depths in a climate model of intermediate complexity with favourable results, although in the absence of direct modelling the waves were parameterised in terms of the wind.

In a later experiment by Babanin and Haus, turbulence was measured using particle image velocimetry (PIV), enabling quantitative measurements. The aim was to directly observe turbulence generated by waves in an otherwise quiescent flume. The PIV was set up to measure just below the troughs, ensuring that it was always measuring on the water side of the interface. In these experiments the critical Reynolds number threshold was not corroborated. Instead, intermittent turbulence was measured at a variety of wave amplitudes, determined by examining the

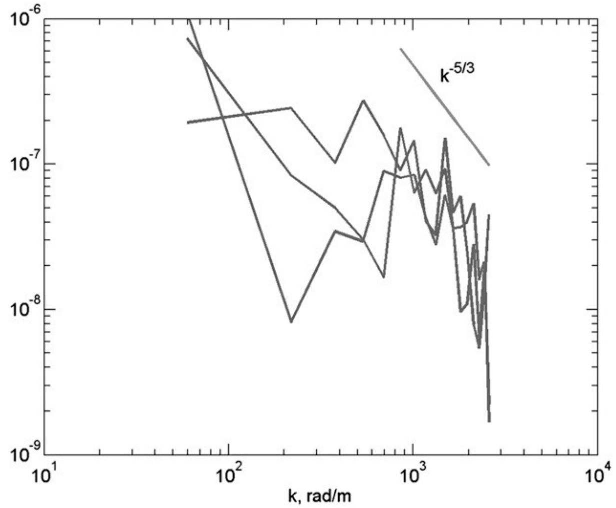

Fig. 4.2. Particle image velocimetry records in wave number space from the wave tank experiment described by Babanin and Haus [2009]. Several velocity spectra from the experiments are shown, appearing to show the Kolmogorov $\kappa^{5/3}$ interval. (In their figure they represent the wave number of the turbulence as k, which we have used elsewhere to represent turbulent kinetic energy.) [Figure from Babanin and Haus, 2009]

velocity spectra (see figure 4.2). Since these results were used to develop the parameterisation in section 5.5, we leave further discussion of the results until then.

The experiment by Dai et al. [2010] was more directly aimed at examining how quickly the waves mixed a stratified fluid. Water was chilled from below and the stably stratified fluid was allowed to sit until the temperature throughout the fluid equilibrated. This process took about 20 hours. Next, from the same initial state of stable stratification, monochromatic waves were generated and the mixing rate measured—now the fluid reached thermal equilibrium in minutes; see figure 4.3. Numerical modelling, based on the B_v model of Qiao et al. [2004] (see section 5.1), agreed reasonably well with the observations. The experimental design featured several problems: shallow water depth, the existence of internal waves due to the stratified fluid, and return currents caused by the Stokes drift, and indeed the effects of stratification on them. In their analysis they addressed these matters in such a way that it seems unlikely that the absence of any of these complications would change the results—the only exception seems to be that any effect of the refrigeration tubes, which lay on the bottom, is unclear.

4.8 Applying new observational techniques

Veron et al. [2009] applied a novel technique using infrared imaging to measure surface kinematics —not just velocities, but divergence, vorticity, shear and normal deformation. The study involved both measuring the naturally evolving surface temperatures and an active method whereby a laser was used to heat spots on the surface in a predictable pattern. The movement of the patterns can be used to characterise the surface turbulence, though of course this does not give the

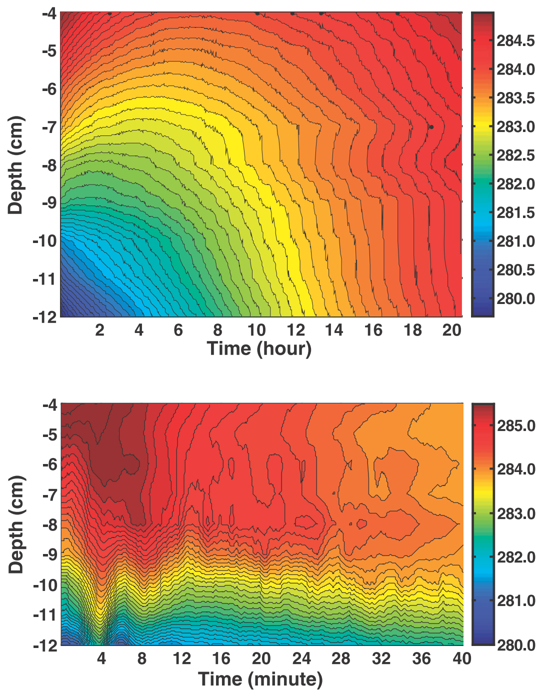

Fig. 4.3. Mixing experiment measurements showing the effect of non-breaking waves on mixing. The upper plot shows the evolution of a stratified fluid with time, measured in hours, while the lower plot shows the much more rapid mixing when surface waves are generated, measured in minutes. The waves are of amplitude 1 cm and wave length of 30 cm. Other effects, such as the return flow, were accounted for. Temperatures are in Kelvin. [Figures from Dai et al., 2010]

full three dimensional picture of the turbulent eddies. They detected Langmuir cells and were able to find a correlation between the wind waves and the surface turbulence, in particular finding a qualitative agreement between their observations and the dynamics predicted by the rapid distortion theory of Teixeira and Belcher [2002]. However they were equivocal about the cause of this, offering that it could be either because of waves stretching vortex lines or because of the wind stress on the windward side of the crest, with the latter explanation suggesting itself from the enhanced turbulence just behind the wave crests. Importantly, they did not find any connection between the turbulence and the swell—perhaps this effect is in general too weak or the specific waves examined here were not steep enough.

Using similar techniques, but in the laboratory, Savelyev et al. [2012] were able to show indeed that without wind the passage of waves lead to a net production of turbulent kinetic energy, where again the observations were limited to measurements of the surface velocities. Also noted by Veron et al. [2009] was that the turbulence was strongly non-homogeneous, an important insight since most commonly used turbulence models carry an assumption of homogeneity, as well as isotropy. In some of the experimental runs the thermal imaging showed elongated eddies

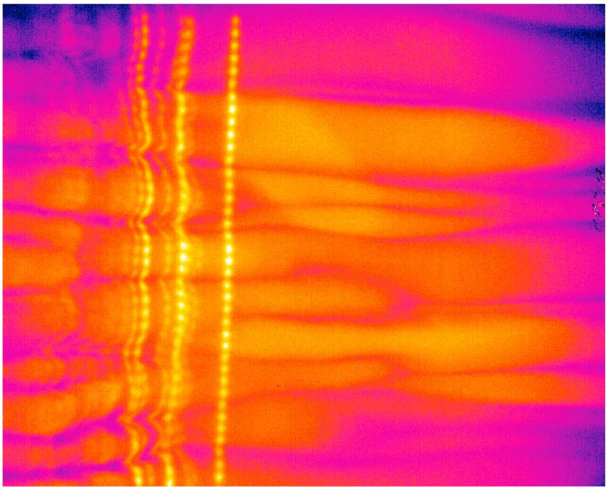

Fig. 4.4. Infrared image from the experiment of Savelyev et al. [2012] showing elongated near-surface eddies as long horizontal structures, as well as the thermal markers generated by laser (vertical line of dots). Waves are propagating from right to left. [Figure from Savelyev et al., 2012]

at the surface, which can be seen in figure 4.4, with streaks not dissimilar to those found by Veron et al., which they had attributed to Langmuir circulation. Here, however, Savelyev et al. explained the streaks in terms of convective cells, and we note again the absence of wind.

Savelyev et al. compared their results with a numerical model, whose details are given by Babanin and Chalikov [2012] and which we discuss here. Since the physics of wave-induced turbulence and wave–turbulence interaction is still not fully understood, despite the revealing analytical work by the likes of Kitaigorodskii and Lumley [1983], Benilov et al. [1993] and Teixeira and Belcher [2002], there is much that can be learned from modelling. Babanin and Chalikov [2012] attempted to simulate the interaction of fully non-linear potential waves with turbulence by forcing a large eddy simulation with the wave model of Chalikov and Sheinin [1998]. This coupled model may be seen as the non-linear extension of Benilov et al.'s [1993] problem for wave-induced growth of vorticity by linear waves. By solving the equations numerically, the growth of energy in the vorticity field—and not just the onset of instability—may be examined thoroughly.

The model successfully reproduced the main feature of the vortex instability theory: vorticity grew under the passage of potential waves, excepting the component aligned with the wave crests (equations (4.31)). The numerical solutions also corresponded qualitatively with laboratory studies, in particular corroborating Babanin and Haus's [2009] observations of intermittent turbulence and turbulence concentrated under the crests—see figure 4.5. (Babanin and Chalikov [2012] went further and claimed that the model showed turbulence concentrated at the rear face of the wave, also observed by Babanin and Haus [2009], but this is not clearly apparent from the figures in the former paper, nor from our own figure 4.5.) Savelyev et al. [2012] also reported good agreement with experiments, particularly with regard to the anisotropic nature of the

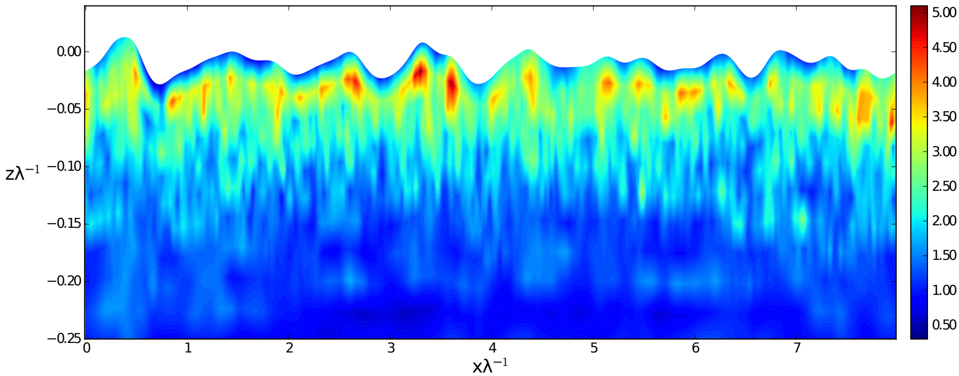

Fig. 4.5. Non-dimensional turbulent kinetic energy (TKE) $k\lambda^{-1}g^{-1}(\times 10^{-6})$, where k is TKE per unit mass and g gravitational acceleration, horizontally averaged in y. Depth z and horizontal distance x are scaled by the peak wavelength λ. This image was produced from output of the model described by Babanin and Chalikov [2012]. The spectrum is a JONSWAP spectrum, but the results should be understood as being qualitative and approximate rather than exact for a particular situation. Note in particular that the TKE is most intense immediately beneath the crests, and sometimes above the level of nearby troughs, yet significant turbulence extends at least as far down as the wave length. The figure was produced by the authors.

turbulence. Although the numerical model allowed them to impose a background vorticity, the experiments relied on whatever existing vorticity there was in the water, which was unknown, so a reliable numerical comparison was out of the scope of the study. Nevertheless, both the model and the experiment showed the same trends of increasing turbulent kinetic energy, and especially a strong dependence of turbulence production on initial turbulence—in other words, just as vertical shear generated turbulence production depends on the existing Reynolds stresses, so too does that generated by waves. Because initial turbulence was not controlled in the experiment, the strength of this dependence, according to Savelyev et al., may account for why they did not observe a correlation between surface turbulent velocities over time and wave steepness.

The model raises some interesting questions: the wave model is potential, so with no vorticity in the fluid it is incapable of generating turbulence. In order to do so the LES had to be initialised with a small random vorticity field. This then grows under the passage of waves, appearing to approach a steady state where the dissipation of turbulent kinetic energy approached the rate of production of non-potential energy. The results were reported to be in quantitative agreement with the experiments of Babanin and Haus [2009], who generated waves on quiescent water and observed intermittent turbulence. But in those experiments the waves of course could not be not purely potential, so why the agreement? To be sure, there is considerable scatter in the data, and the laboratory experiments were performed for a narrow range of monochromatic wave dimensions, so it could be just an overlapping of two distinct production regimes. If potential (by way of straining vortex lines) and non-potential (by way of high Reynolds number rotational flow) production of turbulence are practically identical in scaling and strength then we would expect the laboratory data to show twice the rate of production as the numerical experiments; indeed, the scatter in the data is large enough to entertain this possibility. Until a non-potential model is developed this likely will not be satisfactorily resolved. In the ocean too it is not entirely clear which process would be dominant, for while ocean waves are much larger, and hence wave Reynolds numbers could be much higher, at the same time turbulence is ever present, so we would expect them to grow purely from wave–vortex interaction. Perhaps a repeat of Savelyev et al.'s [2012] experiments with controlled initial vorticity could help solve this problem.

There remain some issues with the LES approach. Our own tests ran for much longer than the tests by Babanin and Chalikov [2012] and we found that the energy did not saturate. This runs counter to the expectation that production of turbulence and its dissipation should eventually reach a steady state, but it may not be an issue if we run it for short enough times. Clearly if the waves are continually generated and pass over a column of water they will continue to add energy, and there is no reason to expect this to be self-limiting without some kind of regime change which the model, presumably, cannot replicate. Modelling is of course never a perfect substitution for direct measurement, but the insight can be invaluable, and while arguably incomplete this model demonstrates a physical mechanism quite clearly. With further refinement there is hope it might enable quantitative prediction of the phenomenon.

4.9 A dissenting view

Although the scholarly community has yet to form a consensus on the question of whether waves can effectively mix the ocean by producing turbulence through their orbital motion, there are few published works which explicitly attempt to show the contrary. Phillips [1961], whose argument we addressed in section 4.2, is the first we're aware of, but a more recent one by Beyá et al. [2012] attempted to reproduce the laboratory experiments of Babanin [2006] and Babanin and Haus [2009]. The results were negative—they could not detect any turbulence in their own laboratory experiments. However it appears that there was some confusion between the rather different experiments by Babanin [2006] and Babanin and Haus [2009], and their experimental findings may indeed be entirely consistent with the findings of both earlier experiments. A more detailed discussion appears in the appendices of Ghantous and Babanin [2014].

5 Recent parameterisations

Over the last decade a number of parameterisations have been proposed and applied to problems involving ocean mixing. In every case improvements in model predictions have been reported despite several theoretical issues remaining. We discuss these parameterisations here.

5.1 B_v

We have devoted a considerable amount of space to discussing B_v since it has been applied to so many studies using different geophysical models and different mixing models, sometimes coupled with atmospheric models, in both climate and weather contexts. We do not quite cover every one of these, but enough to understand its theory, applicability and limitations.

5.1.1 Formulation

Qiao et al. [2004] formulated a new parameterisation for mixing by the waves which they would go on to apply to several different models. They began by considering a further decomposition of the velocity fields to incorporate a wave orbital component (in section 4.6 we described work where this line of theoretical enquiry is taken even further). Recall the velocity decompositions from section 3, which we can expand to include the second horizontal velocity component and scalars:

$$u = U + u', v = V + v', w = W + w', s = S + s'. \tag{5.1}$$

With a wave component we can express the fluctuating velocities as

$$u_i' = u_i^t + u_i^w, \tag{5.2}$$

where the superscript w refers to the wave orbital velocities and t to turbulence. The Reynolds stresses then become

$$-\overline{u_i'u_j'} = -\overline{u_i^w u_j^w} - \overline{u_i^w u_j^t} - \overline{u_i^t u_j^w} - \overline{u_i^t u_j^t}. \tag{5.3}$$

Similarly, the diffusivities of scalars can be written as

$$-\overline{u_i's'} = -\overline{u_i^w s'} - \overline{u_i^t s'}. \tag{5.4}$$

Prandtl's mixing length hypothesis assumes that the turbulent viscosity is proportional to a characteristic velocity scale and a mixing length (by analogy with the mean free path of molecular viscosity),

$$\nu_T = l_m u_c \tag{5.5}$$

where l_m is the mixing length; furthermore it postulates that the characteristic velocity u_c is also proportional to this length,

$$u_c = l_m \left| \frac{\partial U}{\partial z} \right| \tag{5.6}$$

where U is the mean velocity of the flow (at a scale much larger than the turbulence). Thus

$$\nu_T = l_m^2 \left| \frac{\partial U}{\partial z} \right|. \tag{5.7}$$

Qiao et al. associate these terms with characteristic equations for linear waves, so l_m now becomes l_w,

$$l_w \sim \iint_{\boldsymbol{\kappa}} A(\boldsymbol{\kappa}) e^{\kappa z} e^{i(\boldsymbol{\kappa}\cdot\mathbf{x}-\sigma t)} d\boldsymbol{\kappa}. \tag{5.8}$$

$A(\boldsymbol{\kappa})$ is the spectrum of wave amplitudes, so l_w is then proportional to the range of the wave orbitals, which decay with depth via the exponential function. Following the analogy closely we may also determine a characteristic velocity from the wave variance spectrum, $E(\boldsymbol{\kappa})$, so

$$u'_{\text{wave}} = l_w \frac{\partial}{\partial z} \sqrt{\iint_{\boldsymbol{\kappa}} \sigma^2 E(\boldsymbol{\kappa}) e^{2\kappa z} d\boldsymbol{\kappa}}. \tag{5.9}$$

u'_{wave} is the change of vertical wave velocity over the distance of the mixing length l_w, the wave equivalent of equation (5.6). Again using the variance spectrum l_w can be re-expressed as

$$l_w^2 = \alpha \iint_{\boldsymbol{\kappa}} E(\boldsymbol{\kappa}) e^{2\kappa z} d\boldsymbol{\kappa}. \tag{5.10}$$

Following (5.7), a new parameter for wave-induced turbulent viscosity can now be defined, which they call B_v:

$$\nu_{T\text{wave}} = B_v = l_w u'_{\text{wave}} = \alpha \iint_{\boldsymbol{\kappa}} E(\boldsymbol{\kappa}) e^{2\kappa z} d\boldsymbol{\kappa} \cdot \frac{\partial}{\partial z} \sqrt{\iint_{\boldsymbol{\kappa}} \sigma^2 E(\boldsymbol{\kappa}) e^{2\kappa z} d\boldsymbol{\kappa}}, \tag{5.11}$$

with α a constant of proportionality to be determined. A monochromatic version may also be derived, where the vertical velocity of the wave is given by

$$w_w = -i\sigma A e^{\kappa z} e^{i(\boldsymbol{\kappa}\cdot\mathbf{x}-\sigma t)} \tag{5.12}$$

and from which u'_{wave} may be written

$$u'_{\text{wave}} = l_w \frac{\partial}{\partial z} \sqrt{\overline{w_w w_w}} = l_w \sigma A \kappa e^{\kappa z}, \tag{5.13}$$

where the line indicates a time average. Similarly for l_w:

$$\overline{l_w^2} = \alpha A^2 e^{2\kappa z}, \tag{5.14}$$

and finally

$$B_v = \alpha A^3 \kappa \sigma e^{3\kappa z}. \tag{5.15}$$

In order to test the parameterisation, it was introduced into an ocean circulation model—in this case the Princeton Ocean Model (POM), which uses the Mellor–Yamada 2.5 turbulence closure, a type of two-equation model using equations of the form (3.3) and (3.5) (see section 3). The vertical mixing in the ocean model is determined for momentum by a turbulent viscosity ν_m and, for scalars, a diffusivity ν_C, and the Mellor–Yamada closure is used to calculate these from the transport equations via the relations

$$\nu_m = c_\mu l\sqrt{k} \quad and \quad \nu_C = c'_\mu l\sqrt{k} \tag{5.16}$$

where the so-called stability functions c_μ and c'_μ are different for scalars and for momentum. The main feature we wish to point out here is that the eddy viscosity and diffusivity are themselves functions of the TKE and the length scale (determined, in the Mellor–Yamada 2.5 model, by the transport equation for the quantity kl); at the same time, they appear in these transport equations, feeding back on their constituent parameters. In their study, Qiao et al. add B_v to both ν_m and ν_C.

There are two options for where B_v may be added. One option, the one taken by Qiao et al. [2004], is to add it once the turbulence transport equations have been solved, by adding it to the eddy viscosity and diffusivity in the mean flow equations. This, however, means that any feedback effects would be lost. A more serious problem is the fact that eddy viscosities are being added at all—clearly, and this can be seen from studying the two equation models, having an extra source of turbulence is not equivalent to simply adding each source's eddy viscosity calculated in isolation.

Another way would be to add B_v to the eddy viscosity within the turbulent transport equations. This would have the effect of including the feedbacks in the turbulence calculations, but it may have other unanticipated effects on the equations. All turbulence models, to greater or lesser extents, feature empirically defined parameters, so there is nothing inconsistent as such about modifying the way the model works. But now the problem of adding viscosities would be brought inside the turbulence transport equations, only serving to compound the issue.

5.1.2 Modelling the ocean with B_v

With prescribed NCEP reanalysis winds and waves computed from a coupled wave–ocean circulation model, Qiao et al. [2004] estimated the effect of waves on vertical mixing in the ocean by calculating B_v. A threshold value for mixing (ν_T=0.0005 m^2 s^{-1}) was set to determine the maximum depth of effective vertical mixing, which enabled them to determine that the B_v term (on its own in this case) could lead to mixing depths of over 120 m in some cases, 10–30 m being more typical, and mixing being stronger during the winter time. Integrating B_v with the ocean model and comparing the output with the Levitus data [Levitus, 1982] they found closer agreement than without the B_v term; here it needs to be noted that, in general, matching model predictions to climatological mixed layers is not an ideal comparison, though it is promising that the agreement is good. Comparing against climatology is common to many of these studies, so the reader may want to bear this in mind.

B_v was not only added to the Mellor–Yamada closure but to other turbulent closure schemes. Wang et al. [2010] applied it to the KPP scheme of Large et al. [1994] using the ROMS ocean circulation model. Here again, the extra mixing produced by the waves through B_v is added to the mixing coefficients determined by the KPP model for both scalars and momentum. However

KPP works very differently to two-equation models like the Mellor–Yamada level 2.5 closure, which brings its own issues.

In the KPP, which we introduced briefly in section 3, the ocean is divided into upper and lower boundary layers with an interior layer between. The upper boundary layer is where the surface processes are most important, so its parameterisation is quite sophisticated; the eddy viscosity K is given the form, with non-dimensional depth ς (positive downwards),

$$K(\varsigma) = hw(\varsigma)G(\varsigma), \tag{5.17}$$

where $K(\varsigma)$ can represent either the diffusivity of scalars or the eddy viscosity of momentum depending on the definition of the depth-dependent velocity scale w. h is the depth of the boundary layer, and the dimensional depth is equal to $h\varsigma$. Finally $G(\varsigma)$ is a cubic function which gives the shape of the eddy viscosity profile. Monin–Obukhov similarity theory is used to define $w(\varsigma)$ near the surface, and at depth a Richardson number, itself calculated from the mean vertical shear and buoyancy, is used to define the bottom of the upper boundary layer.

Although the precise details do not concern us, it is worth reflecting for a minute on the structure of the parameterisation and some of the implications of the choices made. Again we have the issue of adding viscosities, which is usually inappropriate given the non-linearity of the system. KPP does, perhaps, allow a small amount more freedom here, though, since it is not so closely determined by the physics of the mean flow, instead relying on several bulk values which were, by the authors' own admission, themselves occasionally introduced with little formal justification—a reminder that a lot about ocean physics was then, and is still, unknown. The shape function $G(\varsigma)$ seems, at first glance, to be rather arbitrary. Its cubic coefficients are controlled by the boundary conditions, and it is of course designed to conform to observed eddy viscosity profiles. This may, as a result, have the effect of including a certain amount of wave-induced mixing in the model, for if the effect exists, then field measurements of eddy viscosity profiles will include that contribution, and attempting to model a profile by shape will too. This may account for why in their study Wang et al. [2010] found that a reduced value of 0.3 for the coefficient α in B_v performed better when applied to the KPP, a finding corroborated by Shu et al. [2011] in their one-dimensional tests. Shu et al. [2011] also applied B_v to the KPP in the ocean model MOM4, however for these experiments they did not test different values for α, leaving it equal to 1, nonetheless achieving good results.

We mentioned the dependence on the Monin–Obukhov similarity theory. The assumption that it applies well to the ocean has been challenged by D'Alessio [2002], who concluded that the effect of breaking waves meant that the structure of the upper ocean would diverge from that predicted by Monin–Obukhov theory. Yet at the same time he acknowledged the successful predictions made by the KPP, and suggested that perhaps this was because the influence of breaking was confined to a thin surface layer. We speculate further that it may be that non-breaking waves also affect the Monin–Obukhov theory, and that the improvements seen by Wang et al. [2010] could be made more exact by reformulating the Monin–Obukhov theory used in KPP to take non-breaking waves into account.

Martin et al. [2011] reported on numerical mixing tests simulating buoy measurements using the Mellor–Yamada level 2 closure (as distinct from the two-equation Mellor–Yamada level 2.5 model that Qiao et al. [2004] had used). The model was modified firstly to include the parameterisation by Large et al. [1994] for mixing caused by breaking internal waves at the bottom of the mixed layer. This greatly improved the model's ability to reproduce observed sea surface temperatures in summer, though there was some room for improvement—in particular, some over-predicted spikes remained. Instead of these enhancements, B_v was also tested. Again the predictions of sea surface temperature showed improvement in summer and this time the spikes were removed, but often by too much. More problematic was that B_v led to a too-strong diffusion of the thermocline, which is to say that normally where the thermocline is a clear demarcation between stratified and well-mixed water, presenting as a steep temperature or salinity gradient, with B_v the gradient is greatly reduced. Normally a stratified ocean will tend to inhibit mixing, but since B_v is not dependent on stratification it applies the same diffusion to all parts of the vertical profile. A similar result was also demonstrated by Ghantous and Babanin [2014], though since in those highly idealised tests the waves were assumed to be the only source of mixing the effect was more extreme than would usually be encountered in an ocean prediction context. This issue with B_v could presumably be alleviated if the model's resolution were coarser, and perhaps this explains why the climate-scale studies fared so well. Coarse resolution may also help elsewhere—Ghantous and Babanin [2014] also suggested that B_v's exponential increase of eddy viscosity right up to the surface was unrealistic. Whether or not this is strictly true, in a model of limited vertical resolution this would hardly be a problem. In connection with these issues it is worth noting that Qiao and Huang [2012] found that B_v without vertical shear performed better than vertical shear without B_v, perhaps rendering these issues moot, at least in certain modelling contexts, and additionally indicating that perhaps turbulence from wave orbital motion is not just a useful additional term, but instead the most important one.

5.1.3 Use in coupled models

The application of B_v was not only to ocean models, but also to coupled climate models. Song et al. [2012a] describe a coupled atmospheric and ocean circulation model which enabled feedback from the ocean to the atmosphere. In their simulations they also included a wave model to test the impact of mixing due to non-breaking waves. The mixing model used was that of Pacanowski and Philander [1981], who parameterised eddy viscosity and diffusivity in terms of Richardson numbers:

$$\nu_m = \frac{\nu_0}{(1+\alpha \mathrm{Ri})^n} + \nu_b \tag{5.18}$$

$$\nu_C = \frac{\nu_m}{(1+\alpha \mathrm{Ri})} + \kappa_b, \tag{5.19}$$

where α, ν_0 and n are tuning parameters, ν_b and κ_b are background eddy viscosity and diffusivity, and Ri is the Richardson number,

$$\mathrm{Ri} = \frac{\beta g \frac{\partial \theta}{\partial z}}{\frac{\partial U}{\partial z}^2 + \frac{\partial V}{\partial z}^2} \tag{5.20}$$

with β the coefficient of thermal expansion of water and θ the potential temperature. This parameterisation was intended to be an improvement over constant values for eddy viscosity and diffusivity, and specifically for tropical oceans, but it remains much simpler than the KPP. Because of this simplicity it cannot hope to capture all the physics present in the KPP (and other, more complicated models), but it also means that most of the problems encountered in adding B_v to other mixing schemes are somewhat moot. With all the complexity removed, what remains is a simple scaling based on empirical parameters, and questions such as those about the applicability of Monin–Obukhov theory may be put aside. The question of adding viscosities remains, though.

The focus of Song et al. [2012a] was on the South Asian Summer Monsoon, so a lot of the analysis of model data focussed on atmospheric processes, such as atmospheric flow and water vapour transport. Being a summertime event one might expect that the mixing predicted with the inclusion of waves would make a significant difference, given that models tend to underpredict summertime mixing. Indeed, the results showed quite striking improvements of model fidelity with the inclusion of waves, demonstrating at the same time the importance of the effect of feedback of sea surface temperature on the atmosphere. Similar conclusions were reached by Song et al. [2012b], who focussed on the equatorial eastern Pacific. According to the authors the feedbacks were so important here that including them increased the sea surface temperature in regions where predictions have been known to be too low, such as in the eastern Pacific's cold tongue—the opposite of the drop one might expect from increasing the mixing. But as can be seen from the plots in figure 5.1, model biases were still present, and in the western pacific even exacerbated.

We round off our discussion of B_v with a recent paper by Zhao et al. [2014]. In their study of tropical cyclone tracks they found that a coupled model usually reduced track position errors by a small amount, whereas by further adding in wave-induced mixing with B_v those errors could be reduced by an even greater margin. This improvement was not universal, and B_v actually led to an increase in errors for a number of storms; also, from year to year the improvement could be greater or lesser, however averaged over their database of four years of tropical cyclones in the western Pacific they managed a 7% reduction in errors compared to the coupled model without B_v, and a 9% reduction compared to the control, which featured prescribed sea surface temperatures from NCEP. They also reported that including B_v seemed to be less successful for smaller storms, and suggest that this could be because of issues with model resolution and the difficulty in tracking smaller storms which have more irregular eyes.

5.2 An alternative eddy viscosity parameterisation

Pleskachevsky et al. [2005] included a wave-induced effect in their model for sediment suspension. After sediment is brought into suspension by bottom processes, motion in the water column keeps it suspended. They suggested the following form for the eddy viscosity contribution from the waves,

$$\nu_w = (\kappa H_s)^2 U_{\text{wave}}^2 T, \tag{5.21}$$

where U_{wave} is the mean orbital velocity for waves of the significant wave height, and the depth dependence enters here. This formula is added directly to the eddy viscosity calculated from the mean shear. While this model is dimensionally correct there is no information given as to how it was developed, so it is hard to evaluate its physical meaning. We note that the values for eddy viscosity it produces are about an order of magnitude smaller than those of B_v with $\alpha = 1$.

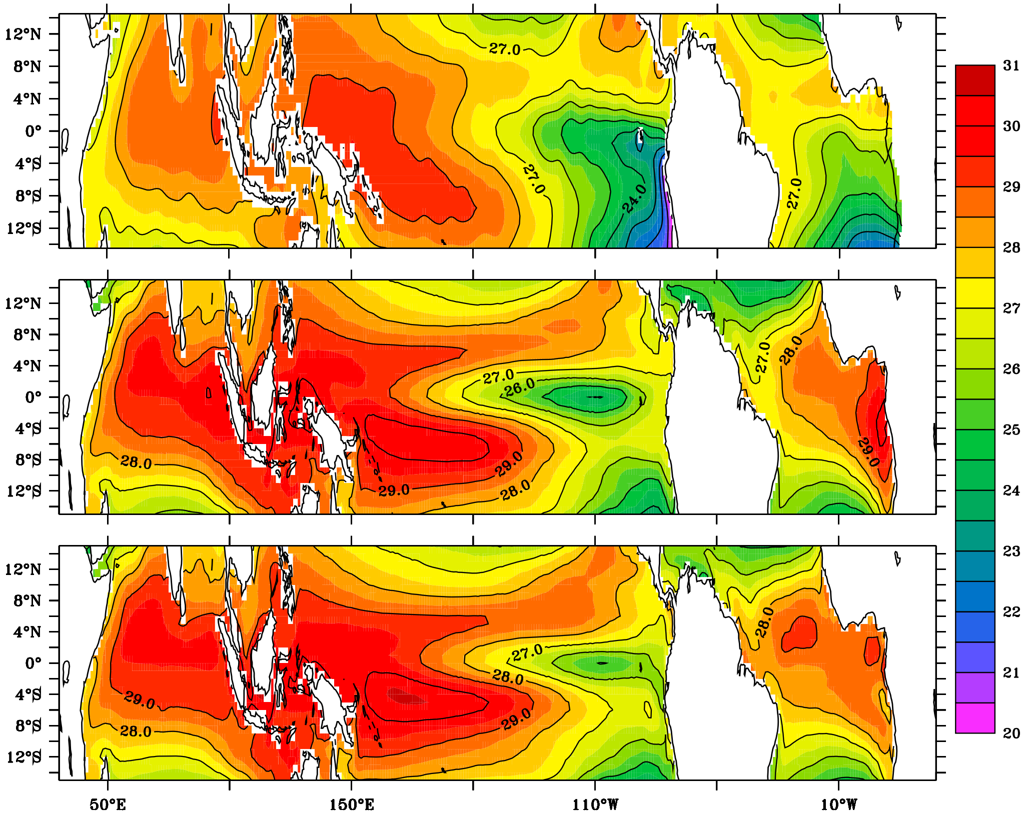

Fig. 5.1. An example of the feedback effects of including the B_v parameterisation in a coupled atmospheric–wave–ocean model. The plots show observed and modelled sea surface temperatures (SSTs). The topmost plot is climatological annual mean SST, the second is modelled without B_v and the third with B_v. Including B_v does in general bring the model closer to the data, especially in the Atlantic and the eastern Pacific where the extra mixing can lead to an increase in SST. The western and northern Pacific seems to fare slightly worse, on the other hand. Temperatures are given in degrees Celcius. [Figure from Song et al., 2012b]

5.3 A Stokes drift production term

Several authors, seeking to invoke non-breaking wave effects in turbulence models, have added the Stokes drift to the mean shear. Sometimes, as with McWilliams et al. [1997] and Kantha and Clayson [2004], the Stokes drift has been used to parameterise Langmuir circulation, which it is believed plays an important role in ocean mixing. Since Langmuir circulation is a subject with its own broad literature we will not attempt to discuss this in great detail, however the parameterisation of Kantha and Clayson [2004] in particular shares some features with some other parameterisations considered here, and a comparison is instructive so we discuss it briefly later on. Qiao et al. [2010] even re-expressed their monochromatic formula for B_v in terms of Stokes drift, though in this case it can be thought of purely as a scaling term. Huang and Qiao

[2010] on the other hand considered turbulence production. Similar to the formula for shear driven turbulence, several authors proposed a formula using Stokes drift:

$$\epsilon = -\overline{u'w'}\frac{\partial u_s}{\partial z}, \tag{5.22}$$

where ϵ is the dissipation rate of TKE and u_s is the stokes drift. In order to parameterise $\overline{u'w'}$ they assumed similarity of the surface layers. With the surface wind stress, τ_{wind}, this leads to

$$-\overline{u'w'} \sim u_*^2 = \frac{\tau_{\mathrm{wind}}}{\rho_w}, \tag{5.23}$$

where ρ_w is the density of water and u_* is the friction velocity in the water. By parameterising the Reynolds stress explicitly in terms of the wind stress this formulation of course leaves out the interaction of the Stokes drift with any other sources of turbulence such as density driven currents or buoyancy effects. The proportionality is dealt with by introducing an empirical parameter, a_1, so that the dissipation of TKE becomes

$$\epsilon_h = a_1 u_*^2 \frac{\partial u_s}{\partial z}. \tag{5.24}$$

Using data from Anis and Moum [1995] they determined that a_1 could be set to

$$a_1 = 3.75\beta\pi\sqrt{\delta}, \tag{5.25}$$

with δ being the steepness defined as H_s/L, and H_s the significant wave height. β is a non-dimensional parameter which depends on which field campaign from Anis and Moum [1995] the formula is applied to.

By using the Stokes drift as the driver for turbulence production by non-breaking waves it is possible that an essential part of the physics is being left out. Given the empirical nature of the parameterisation it is likely that this only affects the precise form of the vertical scaling. But here the TKE dissipation is explicitly dependent on the wind stress, so this model differs fundamentally to the B_v model, which can induce strong mixing even when the wind stress is zero. We note also the somewhat troublingly large variation in the parameter β, which ranged between 0.15 and 1.0. After the thorough analysis by Huang and Qiao [2010], this result is highly instructive: nature does not seem, in this instance, to lend itself to an easy description.

In addition to calculating the dissipation rate, they also refined the B_v formula using the same data from Anis and Moum [1995]. Using one of the field campaigns they determined that

$$\alpha = 10^5 \frac{2u_*^2}{gL}. \tag{5.26}$$

With this they were able to show good agreement between B_v and the Osborne dissipation model, which estimates the rate of mixing based on measured dissipation rates. This is partly a consequence of both models being fitted to the same data, but in this case α is much simpler in form than a_1, and the scaling appears to be more robust. A simple calculation shows that the values for α from the data of Anis and Moum [1995] are much smaller than those assumed by Qiao et al. [2004], Qiao et al. [2010] and other studies, barely exceeding 0.12 and becoming as small as 0.008. Since the wave heights were never more than 3 m, with a wave length of well over 200 m, this could be because in the large scale modelling of the other studies the absence of wave-induced mixing only becomes important for the highest, steepest waves.

Finally, Huang and Qiao [2010] incorporated their model for wave-induced turbulence dissipation into the Mellor–Yamada level 2.5 turbulence closure. Achieving this is more straightforward than with B_v (see section 5.1 for a discussion of the difficulties encountered) since it is simple in a two-equation model to add another source of production. The turbulence dissipation (5.24) is assumed to be equal to the rate of turbulence production, so the wave-induced turbulence production rate is given by

$$P_w = \epsilon_h. \tag{5.27}$$

The Mellor–Yamada 2.5 closure follows the form of the transport equations (3.3) and (3.5), and the shear production term P is modified:

$$P = P_s + P_w, \tag{5.28}$$

where P is now the sum of the production due to shear (P_s) and that due to the waves. Whatever the questions raised by the empirical fitting of the wave parameters their numerical experiments demonstrated that the unmodified model was unable to replicate the observed dissipation rates.

Huang et al. [2011] built on the work of Huang and Qiao [2010] with one-dimensional simulations of the data from Ocean Weather Station Papa and with three-dimensional ocean simulations, again using the Mellor–Yamada 2.5 closure. They concentrated on the boreal summertime where the Mellor–Yamada closure is well known to underestimate mixing [Ezer, 2000]. Alongside the model runs incorporating wave-induced turbulence through equation (5.24), they also performed runs with the wave breaking parameterisation of Craig and Banner [1994] instead of (5.24) [see in particular Mellor and Blumberg, 2004]. In this study β was apparently set to 1. Comparisons with climatology for these latter experiments show clear improvements, though again we must be cautious about using climatology in this way. The comparisons with the OWS Papa data, where daily means are used instead of monthly means as for the climatology, may therefore be more telling. The simulations with (5.24) produced results more faithful to the data between June and October, with differences of up to half a degree of sea surface temperature between the modified and unmodified model; the model with wave breaking was broadly similar to the unmodified data. On the other hand, between November and January the sea surface temperature was over-estimated by the model incorporating the new term. They attributed this to unmodelled three-dimensional effects. Of course during this period of colder surface temperatures convection would play a bigger part, and we note that the control run with the unmodified model, and that with wave breaking, also overestimated the sea surface temperature.

A broadly similar but more complicated picture emerged when they compared mixed layer depths for OWS Papa (though here the precise definition of the mixed layer must have a part to play). Their new parameterisation improved predictions for many periods, though not all. Occasionally the unmodified model performed better (especially in November), and occasionally the model with wave breaking seems to have done best. Through October and November the mixed layer was predicted deeper than observed, but it was the opposite in December and January.

Huang et al. [2012b] [note also Huang et al., 2012a] continued the work begun by Huang and Qiao [2010] by attempting to fit the theoretical prediction (5.24) to newly acquired field data.

The results were broadly similar to those of Huang and Qiao [2010] but with even broader values for β of between 0.20 and 1.5. Since current data was coarse and heat fluxes absent, the authors concluded that more data needed to be collected to properly constrain the parameterisation, and it could be that this would also help determine a more useful form for β.

5.4 A wave mean shear frequency production term

Pleskachevsky et al. [2011] presented a parameterisation which consisted of two components: a production term, and a viscous term.

For vertical shear, the shear frequency M of the mean motion may be defined as

$$M^2 = \left(\frac{\partial U}{\partial z}\right)^2 + \left(\frac{\partial U}{\partial z}\right)^2. \tag{5.29}$$

For unidirectional waves the shear is both vertical and horizontal, and we may define a wave shear frequency M_{wave}, where

$$M_{\mathrm{wave}}^2 = \left(\frac{\partial U_{\mathrm{wave}}}{\partial z}\right)^2 + \left(\frac{\partial W_{\mathrm{wave}}}{\partial x}\right)^2. \tag{5.30}$$

Here U_{wave} and W_{wave} are the horizontal and vertical wave velocities. Taking the mean of M_{wave} over a wavelength gives a mean wave shear frequency which, for finite depth water, takes the simple analytic form

$$\overline{M}_{\mathrm{wave}}^2 = \left(\frac{\kappa\pi H \sinh(\kappa[z+d])}{T\sinh(\kappa d)}\right)^2. \tag{5.31}$$

If one takes the Reynolds average of the Navier–Stokes equations, the production of TKE from the shear of the mean flow is

$$P = \tau_{ij}\frac{\partial U_i}{\partial x_j} \approx \nu_T M^2, \tag{5.32}$$

where the approximation holds provided that the mean vertical motions are negligible (usually the case in geophysical models) and we assume the definition of turbulent viscosity. By substituting the mean wave shear frequency for the shear frequency of the mean flow, Pleskachevsky et al. parameterised the production of TKE due to non-breaking waves as

$$P_{\mathrm{wave}} = \nu_T E_{\mathrm{AM}}^2 \overline{M}_{\mathrm{wave}}^2. \tag{5.33}$$

The term E_{AM}^2 is the ratio of energy lost to the waves and transferred to the turbulence, and is empirical. Thus the production term is based on the assumption that the mean wave shear is an appropriate scaling for the production of energy by waves, but which needs to be reduced by an empirically determined amount. This latter requirement is probably sound, as it is not unreasonable to assume that shear due to the waves is of a somewhat different character to that by mean currents. It also seems likely that phase would be important here but it can't be explicitly represented in this formulation. Unlike mean flow, the periodic nature of waves prevents an easy analysis. The suggested value for E_{AM} was 1.5×10^{-4}, though the authors recommended validation by field studies. Indeed, Ghantous and Babanin [2014] found this value was too small to have any effect on its own, resulting in the model being entirely determined by the viscous term, which we discuss next.

In addition to the production term, a separate parameterisation for an addition to the eddy viscosity was presented. This turns out to be identical to the monochromatic version of B_v, equation (5.15). According to Pleskachevsky et al. [2011] this was added along with the new production term to the k-ϵ closure used in the General Ocean Turbulence Model (GOTM), a one-dimensional mixing model. The k-ϵ model, like Mellor–Yamada level 2.5, is a two equation model, featuring two transport equations, one for TKE and, as its name suggests, one for the dissipation, ϵ. Now we have a new problem: including both an additional eddy viscosity and an additional turbulence production term in a two-equation model double counts the effect of the waves. Normally in these models, the eddy viscosity ν_T is calculated from the TKE and dissipation, themselves calculated from their respective transport equations. These equations are both also functions of that very same eddy viscosity. In trying to directly parameterise the eddy viscosity in terms of the waves one can formulate an approximate mixing scheme without directly representing the physical processes, however once one decides to model these processes in detail the eddy viscosity should return to being simply a function of the flow parameters which define it, being the TKE and a length scale determining parameter (such as the dissipation). If indeed the production term is negligible, then this becomes rather academic, since now we are back to just using B_v, with all the advantages and disadvantages that we described in section 5.1.

This parameterisation was introduced into GOTM and used to model the experiment by Babanin [2006], and the results suggested a good match for the data. By including a sediment suspension model in GOTM they could apply it to sediment transport modelling in the North Sea, again apparently with success (they did not present data showing the model's predictions without the new parameterisations). The parameterisation on its own was also used by Toffoli et al. [2012] to estimate turbulence production by waves under a tropical cyclone, though an effect on the mixed layer depth only becomes apparent for the very highest waves.

5.5 Turbulence production and swell dissipation

By increasing the turbulent kinetic energy a wave train must lose energy, so the process by which the waves enhance mixing in the ocean also contributes to the dissipation of swell. The precise amount of swell dissipation which is due to turbulence production is not known, and other processes, such as wind friction, have been postulated [Ardhuin et al., 2009]. For calculating swell dissipation itself this distinction may not be important, since Young et al. [2013] showed that the parameterisations by Ardhuin et al. [2009] and Babanin [2011]—respectively interpreting the sink of swell energy as entirely by the atmosphere or the ocean—are functionally identical, and can be tuned to fit swell dissipation data. Be that as it may, Babanin [2011] argued that the major sink for swell energy is oceanic turbulence, following broad agreement of laboratory [Babanin and Haus, 2009] and numerical [Babanin and Chalikov, 2012] results. Indeed, if the results of the laboratory experiments of Babanin and Haus [2009] were applied to the ocean without modification then they would generate far too much mixing. Babanin [2011] argued that ocean swell is typically of a much lower steepness, and that this accounts for the difference.

5.5.1 Developing a parameterisation for swell dissipation

The basis of this parameterisation comes from a set of laboratory experiments by [Babanin and Haus, 2009] where the dissipation of turbulent kinetic energy near the surface was measured during the passage of waves (figure 4.2). Just under the troughs they determined a relation for the volumetric dissipation of TKE,

$$\epsilon = ba_0^p, \tag{5.34}$$

where $p = 3.0 \pm 1.0$. When the turbulence was measured the value for b was 300, but turbulence was only observed one in every ten wave periods on average. Because of this intermittency, the value for b was taken to be ten times lower to be correct in the mean (we'll revise this value again shortly). By defining a wave Reynolds number as

$$Re_w = \frac{aV}{\nu} = \frac{a^2\sigma}{\nu} \tag{5.35}$$

they argued that, since the inertial forces scaled with the square of the amplitude, the dissipation rate of energy should scale with the cube of it, thus determining the choice $p = 3$.

Since b is dimensional, a non-dimensional form, b_1, was proposed:

$$b = b_1\kappa\sigma^3. \tag{5.36}$$

To guarantee that the measurements would be made in the water, Babanin and Haus [2009] took their measurements just below the troughs. Babanin [2011] considered this to be approximately the mean surface level. This meant that they could use the exponential decay of surface waves in order to scale the turbulent dissipation with depth. Thus the amplitude a may be expressed instead as a_0e^{kz}, where a_0 is the amplitude at the nominal surface—in actuality just below the troughs. This approximation may not be inconsequential, since Babanin and Chalikov [2012] showed with large eddy simulations that the maximum rates of turbulence production were in the crests. Substituting the amplitude and the expression for b into (5.34) gives

$$\epsilon = b_1\kappa\sigma^3a^3e^{3\kappa z}, \tag{5.37}$$

with z positive upwards. To within a constant, the formula (5.34) is identical to (4.6), although their derivations were different. Clearly the assumptions in equations (5.36) and (4.3) are the crucial steps, although it is noteworthy that the measurements from which (5.34) was determined played no small part. It must not be forgotten, though, that being dimensionally correct does not guarantee the right form, and that different formulations can have the same dimensions—Bowden [1950], Qiao et al. [2004] and Pleskachevsky et al. [2005] all derived completely different and independent forms for eddy viscosity.

In the experiments the frequency was 1.5 Hz, so we have (assuming the deep water dispersion relation) $b_1 = 0.004$. Since the value for b_1 (and b before it) was reduced because of the intermittency of the turbulence, it stands to reason that it depends on just how frequently the laminar flow breaks down into turbulence. Thus it is probably not a constant.

After having developed the depth dependent formula for turbulence dissipation, Babanin [2011] applied it to calculate swell dissipation. This can be done by making the usual assumption of a steady state, where the rate of dissipation of turbulent kinetic energy is equal to its rate of production, and by further assuming that all the energy dissipated by non-breaking waves such as swell goes into turbulence production, and that the energy going back to the atmosphere is negligible in comparison. Integrating with depth we can get the rate of specific dissipation in time per unit surface area,

$$D_a = \frac{1}{\rho_w}\frac{dE}{dt} = \frac{1}{3}b_1 a_0^3 \sigma^3, \tag{5.38}$$

where ρ_w is the density of water, and the energy per unit area of a monochromatic wave train is given by

$$E = \frac{1}{2}\rho_w g a_0^2. \tag{5.39}$$

We can calculate the dissipation per unit area over a distance x, $D_x = \frac{1}{\rho_w} dE/dx$, with

$$D_a = \frac{1}{\rho_w}\frac{dE}{dt} = c_g \frac{1}{\rho_w}\frac{dE}{dx}. \tag{5.40}$$

In deep water, this leads to

$$\frac{1}{\rho_w}\frac{dE}{dx} = \frac{2}{3}b_1 g \kappa^2 a_0^3(x), \tag{5.41}$$

where $a_0(x)$ is now a function of distance. Using (5.39) this gives an expression for the reduction of amplitude (or energy) with distance, and it can be compared with swell dissipation data. Doing this, Babanin [2011] determined that a value for b_1 of 0.002 fit the data better. This value was revised lower again by Young et al. [2013] to 0.0014. The lower values suggest, perhaps, that the much lower steepness of swell leads to the laminar flow breaking down less often (in the wave tank the steepness was as high as around $ak = 0.18$, almost an order of magnitude higher). The situation in the ocean is more complicated than that in the lab, however. Turbulence is always present in the ocean, and we would therefore expect that, via the mechanism of Benilov et al. [1993], the waves would continually interact with it, not generate it sporadically as seen in the tank.

The results of the large eddy simulations by Babanin and Chalikov [2012] appear to shed some light on this picture. In those simulations, the waves are potential waves, so vorticity cannot be generated if the simulation starts with zero vorticity. The simulation must be seeded with small, random fluctuations in the vorticity field, and these then grow with the passage of waves. Still, the turbulence is mostly generated in the crests and advected downward, quickly dissipating. The figures they presented clearly show that the turbulence is not uniform.

5.5.2 Application to a mixing model

The formula (5.37) can be used to calculate turbulence production by monochromatic waves, and if we assume that long swell can be approximated by a monochromatic wave then we can incorporate this into a mixing model. This was done by Ghantous and Babanin [2014] in an attempt to rectify some of the issues they encountered with the earlier parameterisations, being principally the questionable direct addition of eddy viscosities, insensitivity to stratification, the dependence on wind stress and the double counting of production sources and additional eddy viscosity. By using a turbulence closure based on the turbulence transport equations they could add an extra source of turbulence production easily, and equation (5.37) is independent of wind, being determined entirely by wave parameters.

They applied it to a one-dimensional mixing model (GOTM, following Pleskachevsky et al. [2011]), choosing to use the k-ϵ closure, though the procedure is the same for all Reynolds-averaged two-equation models. The production was added directly to the right hand side of equation (3.3), and added to the shear production term P in the second equation (3.5). This is important—by assuming that the wave-induced turbulence behaves like a shear turbulence they implicitly assumed that whatever the closure coefficient for P is in the second, length-scale determining equation, that it must apply equally to the wave-induced term. In their parameterisation for Langmuir circulation, Kantha and Clayson [2004] readjusted these coefficients to account for the large scale of Langmuir cells. Since the second equation is used to determine the macro length scale (i.e. the largest, energy-containing eddies) their modification served to increase the length scale due to turbulence generated by waves (through Langmuir circulation) relative to that of shear-generated turbulence. Ghantous and Babanin [2014] assumed that the effect of Langmuir cells was small, so instead assumed, like all the other parameterisations here, that the shear due to the wave orbitals themselves were somehow or other responsible for the generation of turbulence. Changing this coefficient made a noticeable difference, and may be necessary for accurate predictions, but it did not alter the main thrust of their argument, which was that swell dissipation on its own contained enough energy to deepen the mixed layer of a stratified ocean.

Despite trying to improve on previous work, this formulation has its own weaknesses. To begin with, Ghantous and Babanin [2014] did not validate it against observational data. Furthermore, the value for b_1 was treated as constant, even though it almost certainly isn't. The formula (5.37) is also insensitive to eddy viscosity, whereas turbulence production should be proportional to the Reynolds stresses, as in equation (5.32). To some extent, this last problem is mitigated by what we see from the data presented by Young et al. [2013], where the parameterisation represented the data quite well (figure 5.2). Over large distances and times, perhaps, the variations in background viscosity may not be so important. Regarding b_1, a formula dependent on steepness was suggested:

$$b_1 = 5(a\kappa)^2. \tag{5.42}$$

Substituting in the values for the wave tank experiment, where the steepness reached 0.18, we find that this overestimates b_1 by two orders of magnitude. Given that, we speculate that background viscosity and perhaps a somewhat different dependence on steepness might play a role.

5.5.3 A look back at Bowden

We have already noted that this parameterisation is identical to that presented by Bowden [1950]. This is particularly interesting in light of the fact that Bowden derived the expression by directly substituting eddy viscosity for molecular viscosity in the formula for the viscous dissipation of waves. If we assume that this substitution is valid then we are free to choose a form for the eddy viscosity. Bowden chose the simplest possible form, but, as mentioned above (section 5.5.1)

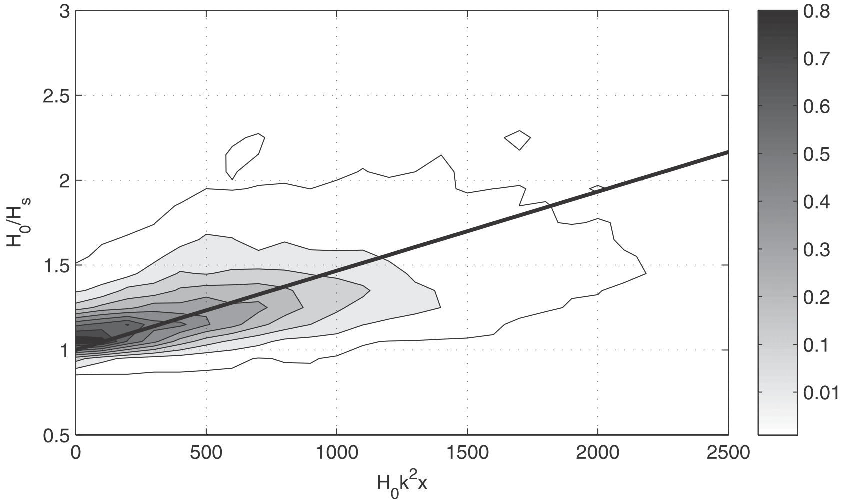

Fig. 5.2. Data showing swell decay measured by altimetry data. H_0 is the original wave height (assumed monochromatic) measured along a great circle path with H_S the subsequently measured height. Contour intervals correspond to the marked intervals on the colourbar and represent data density. The line shows the prediction made using the model of Babanin [2011] with the constant b_1 set to 0.0014. Note that in this figure k is the wave number of the waves. [Figure from Young et al., 2013]

this is not the only possible form for eddy viscosity based on the characteristic scales of waves. Notwithstanding the experimental support for this form by Babanin [2011], this suggests a series of different parameterisations based on the viscous dissipation formula. Recall that Bowden suggested

$$\nu_w \sim a\sigma\kappa^{-1}. \tag{5.43}$$

Pleskachevsky et al.'s [2005] formula, equation (5.21), may be rewritten using the same units,

$$\nu_w \sim a^4\kappa^2\sigma, \tag{5.44}$$

where now the coefficients are left to be determined. Similarly, Qiao et al.'s [2004] parameterisation can be written

$$\nu_w \sim a^3\kappa\sigma. \tag{5.45}$$

We have suppressed the exponential decay in these equations but that may be introduced via the amplitude. By substituting these into (4.4) we can derive alternative forms of equation (4.6), determining the coefficients just as was done by Babanin and Haus [2009] and Babanin [2011], leading to vertical scalings of $e^{3\kappa z}$, $e^{5\kappa z}$ and $e^{6\kappa z}$. While there is no fundamental physical argument for any of these forms—they are all based on dimensional or additionally, in the case of $e^{3\kappa z}$, a similarity argument—it remains an open question which would work best, though Babanin and Haus [2009] make a case for $e^{3\kappa z}$ from their experimental data. It may be that another one not listed here performs better. We must only remember that an eddy viscosity based on wave parameters alone does not accurately represent the component of eddy viscosity produced by waves in an environment with multiple sources of turbulence. This fact poses an uncomfortable observation: the main objection to using an eddy viscosity parameterisation in a mixing model is that eddy viscosities are not additive (so doubling the production of turbulence does not double the eddy viscosity)—yet even the parameterisation for the rate of turbulence production described by Ghantous and Babanin [2014] can be said to implicitly feature some formulation of eddy viscosity, despite eddy viscosities never being directly added. Although there are clear practical advantages in using a production-based parameterisation (such as the preservation of the thermocline) the theoretical implications posed by tying this one to a viscosity representation remain unclear.

6 Lessons from a Langmuir circulation model

Langmuir circulation is not the focus of this review, yet it cannot be left out entirely either since it is a potentially vital contributor to ocean mixing, and it is directly related to waves orbital motion. The first question, whose answer is not immediately clear, is whether the wave-induced turbulence mechanism which is the subject of this review (especially the theoretical results of Benilov et al. [1993], Benilov [2012] and Kitaigorodskii and Lumley [1983]) is entirely distinct from Langmuir circulation. The way we have been thinking about turbulence due to wave orbital motion is that of a localised shear flow—the water particle orbits—imparting energy into the turbulence by stretching vortex lines, while Langmuir circulation is a combination of wave-induced drift interacting with wind induced currents to generate large circulations, which then transport fluid to and from the surface, and they may also bifurcate or generate their own shear turbulence. In this sense these seem to be quite different mechanisms, but ultimately both are a response to waves interacting with other motions in the water, and both can mix the ocean. The theory seems clear—Benilov et al. [1993] and Craik and Leibovich [1976] each provide physical mechanisms for, respectively, vortex instability due to wave orbital motion with no wind stress, nor wave-induced drift, and Langmuir circulation. Under some assumptions, work by McWilliams and Sullivan [2000] and Babanin and Chalikov [2012] suggests that either mechanism without the other is capable of contributing significantly to mixing the ocean. Parameterising these can be complicated because comparisons with data are not always, if at all, capable of distinguishing between them. So what to do? At the moment the unsatisfactory answer is that more work is required on this front. Large eddy simulations such as those by McWilliams and Sullivan [2000] do not incorporate the full orbital motion of the waves, while those of Babanin and Chalikov [2012] do not factor in wind stress. It is quite possible that the two mechanisms together do not combine to form a much greater source of mixing than either one alone, and the difference may be academic.

We do not have a solution to the problem right now. But an increasingly popular mixing model incorporating Langmuir circulation is worth investigating (even superficially as we do here) for a slightly different reason, being that there are aspects of its implementation which should inform any modification to an ocean mixing scheme. Kantha and Clayson's [2004] model was developed to reproduce the results of large eddy simulations by McWilliams et al. [1997], and it has found its way into geophysical models such as the Naval Research Laboratory's COAMPS hurricane prediction model [Allard et al., 2012]. The model is derived by first adding a Stokes drift term to the equations of motion, both for the mean flow and the turbulent kinetic energy. The transport equation for TKE in a geophysical model is given as (3.3), with the usual form for the term P (denoting production of TKE due to mean shear) being

$$P = \overline{u'w'}\frac{\partial U}{\partial z} + \overline{v'w'}\frac{\partial V}{\partial z}. \tag{6.1}$$

The Reynolds stresses may be parameterised as per the first equation of (3.1). By adding Stokes drift, now the equation for P looks like this

$$P = \overline{u'w'}\left(\frac{\partial U}{\partial z} + \frac{\partial U_s}{\partial z}\right) + \overline{v'w'}\left(\frac{\partial V}{\partial z} + \frac{\partial V_s}{\partial z}\right), \tag{6.2}$$

where U_s and V_s are the two horizontal components of Stokes drift. There are some interesting differences between this expression and other parameterisations for wave-induced turbulence production. The waves are entirely represented by the Stokes drift, so certainly, when compared with the decompositions of Kitaigorodskii and Lumley [1983] and Anis and Moum [1995], and the linear waves of Benilov et al. [1993], it is clear that not all of the physics is being represented. We may even say that at this point it hard to connect this to Langmuir circulation at all. But in other respects the revised formula is an elegant and simple modification to the original, and it retains the important property of having the turbulence production rate depend on the magnitude of the turbulence. Another property worthy of note is that the Stokes drift may be directed differently to the mean currents, and if opposed to the currents will result in a reduction of turbulence production. This is the opposite of what we'd expect from the full wave orbital motion interacting with the turbulence, but it does beg the question: how indeed do the wave orbitals interact with an oppositely directed current? Or in cross swell or multimodal spectra? More specifically, how is *turbulence* generated by wave orbital motion from a multimodal spectrum affected?

The second equation brings another innovation. The Mellor–Yamada second equation may be written

$$\frac{Dq^2l}{Dt} - \frac{\partial}{\partial z}\left(qlS_1\frac{\partial q^2 l}{\partial z}\right) = E_1 l\left(-\overline{u'w'}\frac{\partial U}{\partial z} - \overline{v'w'}\frac{\partial V}{\partial z}\right) + E_3\beta g\overline{w'\theta'} - E_2\frac{q^3}{B_1}\left(1 + E_4\left(\frac{l}{\kappa_{\mathrm{vK}} l_w}\right)^2\right) + E_5 2\Omega q^2 l. \quad (6.3)$$

Since Kantha and Clayson tasked themselves with modifying the Mellor–Yamada turbulence closure we use here the notation most usually associated with that model, so some explanation is necessary. (While these equations can in principle be expressed in terms of the generic model (3.5) the modifications were specific to the Mellor–Yamada closure and translating to another closure would require some work.) Mellor and Yamada [1982] preferred the notation q^2 for the turbulent kinetic energy instead of k, so in their k-kl model the second, length scale determining equation is for q^2l, where q is the characteristic velocity scale and l is the corresponding length scale, being the scale of the large, energy-containing eddies. β is the coefficient of thermal expansion, θ' is the fluctuation of potential temperature, 2Ω is the Coriolis force, l_w is the distance from the surface and κ_{vK} is the von Kármán constant (though unnecessary in other two-equation models this term was added to the q^2l equation in order to reproduce law-of-the-wall behaviour). We're left with the constants E_1 through E_5, B_1 and S_1 (another constant appears in the kinetic energy equation). The revised equation with the Stokes drift components adds an extra term to the right-hand side,

$$E_6 l\left(-\overline{u'w'}\frac{\partial U_s}{\partial z} - \overline{v'w'}\frac{\partial V_s}{\partial z}\right). \quad (6.4)$$

In order to reproduce the results of the large eddy simulations with Langmuir circulation by McWilliams et al. [1997], E_6 was set to 4 (in fact, this should be even higher [Philip Chu, private communication]), rather higher than any of E_1 through E_5—E_1, for example, is set to 1.8. The interpretation for this larger value is of interest: since this transport equation controls, through q^l, the length scale l of the energy-containing eddies, Kantha and Clayson set a larger E_6 for the Stokes drift terms to reflect the large size of the Langmuir cells. While this was intended to help match the large eddy simulations, the idea is of interest when thinking about models such as that of Huang and Qiao [2010] and Ghantous and Babanin [2014], where the production term is modified but no other closure coefficients are touched. One is entitled to ask whether an appropriate length scale modification should be made for these models too, since wave orbital motion may generate turbulent eddies of a different scale again.

This model for Langmuir circulation was further developed by Harcourt [2013], who paid particular attention to the stability functions. Kantha and Clayson [2004] had used stability functions derived by taking into account shear and buoyancy but without any explicit connection to Langmuir turbulence. Harcourt argued that if the transport equations now feature terms calculated from the Stokes drift, then so should the stability functions. This again is a useful reminder that just including an extra source of turbulence production may not be enough, and that the work of Ghantous and Babanin [2014], Huang and Qiao [2010], and indeed all other attempts to include wave-induced turbulence in such a model, may benefit from similar attention. This is not trivial—a look at the GOTM documentation [Umlauf et al., 2011] shows numerous options for the stability functions, from constants to quite complicated formulas for higher order closure schemes.

Another refinement by Harcourt was to differentiate between the eddy viscosity used to parameterise the Reynolds stresses due to the Stokes shear and those due to mean shear from currents. This is slightly reminiscent of Pleskachevsky et al.'s [2011] modified eddy viscosity, but they applied that eddy viscosity to all aspects of the flow. Instead, Harcourt's approach merely argues that the production due to Stokes drift diffuses differently to that of mean shear.

Another paradigm is suggested by these formulas: that perhaps Stokes drift is enough to characterise the turbulence due to the waves even if, strictly speaking, much of the physics is left out. After all, the same thing is done in Reynolds-averaged turbulence closures themselves, where the mean flow is explicitly defined but the turbulence is parameterised with some rather large assumptions which do not always represent the physics. This doesn't stop these models from working well in many situations, and so it may be said of efforts to represent Langmuir circulation in them. Of course, we must always prefer a full understanding of the physics to a partial one, but for practical purposes something less usually has to suffice.

7 Going forth

If reading this far has left the reader slightly uncomfortable with the present state of the subject then that is a good thing, since it is our view that there are some crucial unsolved problems, and still much work to be done. It's hard to believe after a century of scholarly discourse, but the physics has still not been completely settled—though it has to be admitted that the discourse was rather sparsely spread for many decades. The modelling of Babanin and Chalikov [2012] and the analyses of Benilov et al. [1993] and Nielsen et al. [2011] have probably given the closest to solid theoretical results, but these are not general enough to cover the full range of wave–turbulence interactions. Benilov et al.'s [1993] analysis especially can only hope to show us the existence of an interaction, but it cannot quantify it, and the large eddy simulations are problematic for technical reasons [Dmitry Chalikov, private communication]; neither takes into account non-potential waves.

Experimental work has been limited by a narrow range of wave properties, large scatter in the measurements, apparatus size and measurement precision. Beyond demonstrating existence and broad quantitative estimates, it is not enough to enable us to extrapolate the results to the ocean with great confidence. While correlation does not prove cause, the parameterisations do at least seem to work, albeit imperfectly, especially in climatological contexts. Still, there is no way at present to represent mixing due to wave orbital motion in a model in a way which is solidly based on a physical understanding of the process. The Reynolds-averaged turbulence models need a production term which takes into account all of the physics of wave–turbulence interactions, and their closure coefficients recalibrated. So far this seems like the easiest way to proceed, since models such as the KPP need an altogether more involved approach, where several aspects of the model need to be reformulated: the Richardson number at the edge of the boundary layer needs to take into account a wave effect, and at the surface nothing less than a revision of the Monin–Obukhov similarity theory for the ocean is required.

With so many open questions there isn't much to recommend one of the various parameterisations discussed in section 5 over another, since they are all somewhat reliant on guesswork. For now performance remains the decider, and a comprehensive comparison of them might be a fruitful endeavour. The question of Langmuir circulation cannot be ignored either. Determining the relative contributions of the two mechanisms, if in fact they are entirely separate, should be a priority. Measuring turbulence in the open ocean for extended periods is tremendously difficult, but with research into new techniques, such as running pulse-coherent Doppler sonars from a mooring [Farrar, 2011], and the infrared imaging used by Veron et al. [2009], there is hope for more and better direct observation. And modifying existing turbulence closures might not be enough, the models they're used in may need recalibration themselves.

In addition to these broad questions, there are some specific problems which need to be addressed, such as boundary conditions in models. The GOTM mixing model provides options for the surface boundary condition, but it is unclear which (if either) is best suited to wave-induced turbulence. In their turbulence production-based parameterisation, Ghantous and Babanin [2014] made the choice rather arbitrarily.

Another problem is dependence of the rate of production of turbulence on the Reynolds stresses. A parameterisation should ideally depend on eddy viscosity, such as is done with the Langmuir circulation parameterisation of Kantha and Clayson [2004]. The approach of Pleskachevsky et al. [2011] does feature such a dependence, but it is unverified (indeed, that production term is negligible). The approach of Ghantous and Babanin [2014] has no dependence, even though it is to some extent based on observations. These observations, of swell dissipation, should show a dependence on the level of oceanic turbulence, but if they do it is hard to see. There are two likely reasons for this: the first is that the dependence could be blurred over the scale of the wave dissipation, which is of the order of hundreds or thousands of kilometres. The second is that the dependence might be negligible, at least over the time scales that are important in ocean climate modelling, but if this is the case it has not been demonstrated conclusively anywhere. Some work with the model of Babanin and Chalikov [2012] confirms that the dependence exists and is strong, since the production of turbulence is greater when the initial random turbulence field is greater [Savelyev et al., 2012].

Despite these problems, we feel that the evidence quite strongly supports the existence of non-breaking surface waves as a significant contributor to ocean mixing. This is something that oceanographers of an earlier era and engineers seem to have accepted almost as being obvious, but in latter years has become rather unfashionable. With the surge in attention over the last decade it seems that this trend has reversed, and we anticipate not too far away the emergence of solutions to at least some of the outstanding problems.

Acknowledgements

We would like to thank Dmitry Chalikov for his help in working with the coupled wave–LES model and for useful discussions with him. We are indebted to Anna Babanina for her posthaste translation into English of the article by Dobroklonskiy, and to Lidong Cui for translating for us the papers by Cao and Ma. For a thorough reading of the manuscript and helpful comments we must also thank Fangli Qiao, and Jeff Book and Will Phillips also provided vital advice in specific areas. We extend our thanks to the editor and an anonymous reviewer for their careful reading and constructive criticism. This research was supported by the Australian Research Council (ARC Discovery grant DP130100227).

References

Richard A. Allard, Travis A. Smith, Tommy G. Jensen, Philp Y. Chu, Erick Rogers, Timothy J. Campbell, Uriah M. Gravois, Suzanne N. Carroll, Kim Watson, and Saša Gaberšek. Validation test report for the coupled ocean/atmosphere mesoscale prediction system (COAMPS) version 5.0: Ocean/wave component validation. Technical report, Naval Research Laboratory, Oceanographic Division, Stennis Space Centre, Mississippi, 2012.

A. Anis and J. N. Moum. Surface wave–turbulence interactions: scaling $\epsilon(z)$ near the sea surface. *Journal of Physical Oceanography*, 25(9):2025–2045, 1995.

Fabrice Ardhuin, Bertrand Chapron, and Fabrice Collard. Observation of swell dissipation across oceans. *Geophysical Research Letters*, 36:L06607, 2009. doi: 10.1029/2008GL037030.

A. V. Babanin. On a wave-induced turbulence and a wave-mixed upper ocean layer. *Geophysical Research Letters*, 33:L20605, 2006. doi: 10.1029/2006GL027308.

Alexander Babanin. *Breaking and Dissipation of Ocean Surface Waves*. Cambridge University Press, 2011.

Alexander V. Babanin and Dmitry Chalikov. Numerical investigation of turbulence generation in non-breaking potential waves. *Journal of Geophysical Research*, 117:C00J17, 2012. doi: 10.1029/2012JC007929.

Alexander V. Babanin and Brian K. Haus. On the existence of water turbulence induced by nonbreaking surface waves. *Journal of Physical Oceanography*, 39(10):2675–2679, 2009.

Alexander V. Babanin, Andrey Ganopolski, and William R. C. Phillips. Wave-induced upper-ocean mixing in a climate model of intermediate complexity. *Ocean Modelling*, 29(3):189–197, 2009.

Alexander V. Babanin, Miguel Onorato, and Fangli Qiao. Surface waves and wave-coupled effects in lower atmosphere and upper ocean. *Journal of Geophysical Research*, 117:C00J01, 2012. doi: 10.1029/2012JC007932.

Jurjen Anno Battjes and J. van Heteren. *Measurements of Wind Wave Kinematics*. Rijkswaterstaat, Directie Waterhuishouding en Waterbeweging, 1983.

A. Y. Benilov. On the turbulence generated by the potential surface waves. *Journal of Geophysical Research*, 117:C00J30, 2012.

A. Y. Benilov, T. G. McKee, and A. S. Safray. On the vortex instability of linear surface wave. *Numerical Methods in Laminar & Turbulent Flow VIII, Pineridge Press, UK*, pages 1323–1334, 1993.

J. F. Beyá, W. L. Peirson, and M. L. Banner. Turbulence beneath finite amplitude water waves. *Experiments in Fluids*, 52:1319–1330, 2012.

J. Boussinesq. Essai sur la théorie des eaux courantes. *Mémoires présentés par divers savants à l'Académie des Sciences*, XXIII(1):1–680, 1877.

K. F. Bowden. The effect of eddy viscosity on ocean waves. *Philosophical Magazine*, 41(320): 907–917, 1950.

Zude Cao. Theory of wave-induced turbulence. *Transactions of Tianjin University*, 1962. Partially translated by Lidong Cui, 2014, for the Centre of Ocean Engineering, Science and Technology.

Luigi Cavaleri and Sefano Zecchetto. Reynolds stresses under wind waves. *Journal of Geophysical Research*, 92(C4):3894–3904, 1987.

D. Chalikov and D. Sheinin. Direct modeling of one-dimensional nonlinear potential waves. In W. Perrie, editor, *Nonlinear Ocean Waves, Advances in Fluid Mechanics, vol. 17*, pages 207–258. Computational Mechanics, 1998.

Peter D. Craig and Michael L. Banner. Modeling wave-enhanced turbulence in the ocean surface layer. *Journal of Physical Oceanography*, 24(12):2546–2559, 1994.

A. D. D. Craik and S. Leibovich. A rational model for Langmuir circulations. *Journal of Fluid Mechanics*, 73(3):401–426, 1976.

Dejun Dai, Fangli Qiao, Wojciech Sulisz, Lei Han, and Alexander Babanin. An experiment on the nonbreaking surface-wave-induced vertical mixing. *Journal of Physical Oceanography*, 40(9):2180–2188, 2010.

J. D. D'Alessio. Concerning the influence of wave breaking on Monin-Obukhov similarity theory. *Acta Mechanica*, 157:1–14, 2002.

Eric A. D'Asaro. Turbulence in the upper-ocean mixed layer. *Annual Review of Marine Science*, 6:101–115, 2014.

Raju Datla. *Interactions Between Submerged Turbulence and Surface Waves—A Laboratory Study*. PhD thesis, Stevens Institute of Technology, Hoboken, New Jersey, 1996.

S. V. Dobroklonskiy. Eddy viscosity in the surface layer of the ocean and waves. *Doklady Academii Nauk SSSR*, 58(7):1345–1348, 1947.

Tal Ezer. On the seasonal mixing layer simulated by a basinscale ocean model and the Mellor-Yamada turbulence scheme. *Journal of Geophysical Research*, 105(C7):16843–16855, 2000.

J. Thomas Farrar. Moored turbulence measurements in the open ocean using pulse-coherent doppler sonar. *Journal of Ocean Technology*, 6(2):66–67, 2011.

J. R. D. Francis, H. Stommel, H. G. Farmer, and D. Parson, Jr. Observations of turbulent mixing processes in a tidal estuary. Technical report, Woods Hole Oceanographic Institution, Woods Hole, Massachusetts. Submitted to the Office of Naval Research, 1953.

Malek Ghantous and Alexander V. Babanin. One-dimensional modelling of upper ocean mixing by turbulence due to wave orbital motion. *Nonlinear Processes in Geophysics*, 21(1):325–338, 2014. doi: 10.5194/npg-21-325-2014.

Theodore Green and See Whang Kang. Long-wave decay due to convective turbulence. *Journal of Fluid Mechanics*, 73(3):427–444, 1976.

Theodore Green, Herman Medwin, and James E. Paquin. Measurements of surface wave decay due to underwater turbulence. *Nature*, 237(77):115–117, 1972.

P. Groen and R. Dorrestein. Ocean swell: its decay and period increase. *Nature*, 165(4194): 445–447, 1950.

Ramsey R. Harcourt. A second moment closure model of Langmuir turbulence. *Journal of Physical Oceanography*, 43:673–697, 2013. doi: 10.1175/JPO-D-12-0105.1.

Chuan Jiang Huang and Fangli Qiao. Wave–turbulence interaction and its induced mixing in the upper ocean. *Journal of Geophysical Research*, 115, 2010. doi: 10.1029/2009JC005853.

Chuan Jiang Huang, Fangli Qiao, Dejun Dai, Hongyu Ma, and Jingsong Guo. Correction to "Field measurement of upper ocean turbulence dissipation associated with wave-turbulence interaction in the South China Sea". *Journal of Geophysical Research*, 117(C00J99), 2012a. doi: 10.1029/2012JC008230.

Chuan Jiang Huang, Fangli Qiao, Dejun Dai, Hongyu Ma, and Jingsong Guo. Field measurement of upper ocean turbulence dissipation associated with wave-turbulence interaction in the South China Sea. *Journal of Geophysical Research*, 117(C00J09), 2012b. doi: 10.1029/2011JC007806.

C.J. Huang, F. Qiao, Z. Song, and T. Ezer. Improving simulations of the upper ocean by inclusion of surface waves in the mellor-yamada turbulence scheme. *J. Geophys. Res*, 116, 2011. doi: 10.1029/2010JC006320.

Clifford A. Jacobs. Numerical simulations of the natural variability in water temperature during BOMEX using alternative forms of the vertical eddy exchange coefficients. *Journal of Physical Oceanography*, 8:119–141, 1978a.

Clifford A. Jacobs. Observed oceanic variability at and near the air-sea interface during Phase III of Project BOMEX. *Journal of Physical Oceanography*, 8:103–118, 1978b.

Harold Jeffreys. On turbulence in the ocean. *The London, Edinburgh, and Dublin Philosophical Magazine and Journal of Science*, 39(233):578–586, 1920.

Lakshmi H. Kantha and Carol Anne Clayson. On the effect of surface gravity waves on mixing in the oceanic mixed layer. *Ocean Modelling*, 6(2):101–124, 2004.

Kakani Katija and John O. Dabiri. A viscosity-enhanced mechanism for biogenic ocean mixing. *Nature*, 460:624–626, 2009. doi: 10.1038/nature08207.

Blair Kinsman. *Wind waves*. Prentice-Hall, 1965.

S. A. Kitaigorodskii and J. L. Lumley. Wave–turbulence interactions in the upper ocean. part I: The energy balance of the interacting fields of surface wind waves and wind-induced three-dimensional turbulence. *Journal of Physical Oceanography*, 13:1977–1987, 1983.

S. A. Kitaigorodskii, M. A. Donelan, J. L. Lumley, and E. A. Terray. Wave–turbulence interactions in the upper ocean. part II: Statistical characteristics of wave and turublent components of the random velocity field in the marine surface layer. *Journal of Physical Oceanography*, 13:1988–1999, 1983.

V. N. Kudryatsev and V. K Makin. The impact of air-flow separation on the drag of the sea surface. *Boundary-Layer Meteorology*, 98:155–171, 2001.

Horace Lamb. *Hydrodynamics*. Dover, 1932.

W.G. Large, J.C. McWilliams, and S.C. Doney. Oceanic vertical mixing: A review and a model with a nonlocal boundary layer parameterization. *Reviews of Geophysics*, 32(4):363–403, 1994. ISSN 8755-1209.

Sydney Levitus. Climatological atlas of the world ocean. Technical Report NOAA Prof. Paper 13, NOAA, 1982.

Michael S. Longuet-Higgins. Mass transport in water waves. *Philosophical Transactions of the Royal Society of London. Series A, Mathematical and Physical Sciences*, 245(903):535–581, 1953.

Deshan Ma. Turbulence beneath waves and its parameterization. *Transactions of Tianjin University*, 21, 1965. Partially translated by Lidong Cui, 2014, for the Centre of Ocean Engineering, Science and Technology.

Paul J. Martin, Erick Rogers, Rick A. Allard, Patrick J. Hogan, and James G. Richman. Results from tests of direct wave mixing in the ocean's surface mixed layer. Technical Report NRL/FR/7322-03-10,045, Naval Research Laboratory, Washington, DC, 2011.

James C. McWilliams and Peter P. Sullivan. Vertical mixing by Langmuir circulations. *Spill Science & Technology Bulletin*, 6(3/4):225–237, 2000. ISSN 1353-2561.

James C. McWilliams, Peter P. Sullivan, and Chin-Hoh Moeng. Langmuir turbulence in the ocean. *Journal of Fluid Mechanics*, 334(1):1–30, 1997.

George Mellor and Alan Blumberg. Wave breaking and ocean surface layer thermal response. *Journal of Physical Oceanography*, 34:693–698, 2004.

George L. Mellor and Tetsuji Yamada. Development of a turbulence closure model for geophysical fluid problems. *Reviews of Geophysics and Space Physics*, 20:851–875, 1982.

Jerome H. Milgram. Short wave damping in the simultaneous presence of a surface film and turbulence. *Journal of Geophysical Research*, 103(C8):15717–15727, 1998.

S. G. Monismith, E. A. Cowen, H. M. Nepf, J. Magnaudet, and L. Thais. Laboratory observations of mean flows under surface gravity waves. *Journal of Fluid Mechanics*, 573:131–147, 2007. doi: 10.1017/S0022112006003594.

Peter Nielsen, David P. Callaghan, and Tom E. Baldock. Downward transfer of momentum by wind-driven waves. *Coastal Engineering*, 58:1118–1124, 2011.

Hasan S. Ölmez and Jerome H. Milgram. An experimental study of attenuation of short water waves by turbulence. *Journal of Fluid Mechanics*, 239(1):133–156, 1992.

R. C. Pacanowski and S. G. H. Philander. Parameterization of vertical mixing in numerical models of tropical oceans. *Journal of Physical Oceanography*, 11:1443–1451, 1981.

O. M. Phillips. The scattering of gravity waves by turbulence. *Journal of Fluid Mechanics*, 5: 177–192, 1959.

O. M. Phillips. A note on the turbulence generated by gravity waves. *Journal of Geophysical Research*, 66(9):2889–2893, 1961.

W. R. C. Phillips, A. Dai, and K. K. Tjan. On Lagrangian drift in shallow-water waves on moderate shear. *Journal of Fluid Mechanics*, 660:221–239, 2010. doi: 10.1017/S0022112010002648.

Andrey Pleskachevsky, Gerhard Gayer, Jochen Horstmann, and Wolfgang Rosenthal. Synergy of satellite remote sensing and numerical modeling for monitoring of suspended particulate matter. *Ocean Dynamics*, 55(1), 2005. doi: 10.1007/s10236-004-0101-z.

Andrey Pleskachevsky, Mikhail Dobrynin, Alexander V. Babanin, Heinz Günther, and Emil Stanev. Turbulent mixing due to surface waves indicated by remote sensing of suspended particulate matter and its implementation into coupled modeling of waves, turbulence and circulation. *Journal of Physical Oceanography*, 41:708–724, 2011. ISSN 1520-0485.

Fangli Qiao and Chuan Jiang Huang. Comparison between vertical shear mixing and surface wave-induced mixing in the extratropical ocean. *Journal of Geophysical Research*, 117 (C00J16), 2012. doi: 10.1029/2012JC007930.

Fangli Qiao, Yeli Yuan, Yongzeng Yang, Quanan Zheng, Changshui Xia, and Jian Ma. Wave-induced mixing in the upper ocean: Distribution and application to a global ocean circulation model. *Geophysical Research Letters*, 31:L11303, 2004. doi: 10.1029/2004GL019824.

Fangli Qiao, Yeli Yuan, Tal Ezer, Changshui Xia, Yongzeng Yang, Xiangang Lü, and Zhenya Song. A three-dimensional surface wave–ocean circulation coupled model and its initial testing. *Ocean Dynamics*, 60:1339–1355, 2010.

O. Reynolds. An experimental investigation of the circumstances which determine whether the motion of water shall be direct or sinuous and the law of resistance in parallel channels. *Philosophical Transactions of the Royal Society*, 174:935–982, 1883.

Lewis F. Richardson and Henry Stommel. Note on eddy diffusion in the sea. *Journal of Meteorology*, 5:238–240, 1948.

Ivan B. Savelyev, Eric Maxeiner, and Dmitry Chalikov. Turbulence production by nonbreaking waves: Laboratory and numerical simulations. *Journal of Geophysical Research*, 117:C00J13, 2012. doi: 10.1029/2012JC007928.

David H. Shonting. A preliminary investigation of momentum flux in ocean waves. *Pure and Applied Geophysics*, 57(1):149–152, 1964.

David H. Shonting. Observations of reynolds stresses in wind waves. *Pure and Applied Geophysics*, 81(1):202–210, 1970.

Qi Shu, Fangli Qiao, Zhenya Song, Changshui Xia, and Yongzeng Yang. Improvement of MOM4 by including surface wave-induced vertical mixing. *Ocean Modelling*, 40:42–51, 2011. doi: 10.1016/j.ocemod.2011.07.005.

J. D. Skoda. *The interaction of waves and turbulence in water.* PhD thesis, University of California, Berkeley, 1972.

Yajuan Song, Fangli Qiao, and Zhenya Song. Improved simulation of the South Asian Summer Monsoon in a coupled GCM with a more realistic ocean mixed layer. *Journal of the Atmospheric Sciences*, pages 1681–1690, 2012a. doi: 10.1175/JAS-D-11-0235.1.

Zhenya Song, Fangli Qiao, and Yajuan Song. Response of the equatorial basin-wide SST to non-breaking surface wave-induced mixing in a climate model: An amendment to tropical bias. *Journal of Geophysical Research*, 117(C00J26), 2012b. doi: 10.1029/2012JC007931.

Louis St. Laurent, Matthew H. Alford, and Terri Paluszkiewicz. An introduction to the special issue on internal waves. *Oceanography*, 25(2):15–19, 2012. doi: http://dx.doi.org/10.5670/oceanog.2012.37.

C. T. Suthons. *The forecasting of sea and swell waves*. Naval Meteorological Branch, Hydrographic Department, 1945.

H. U. Sverdrup. Period increase of ocean swell. *Transactions, American Geophysical Union*, 28 (3):407–417, 1947.

M. A. C. Teixeira and S. E. Belcher. On the distortion of turbulence by a progressive surface wave. *Journal of Fluid Mechanics*, 458:229–267, 2002.

S. A. Thorpe. Langmuir circulation. *Annual Review of Fluid Mechanics*, 36:55–79, 2004. doi: 10.1146/annurev.fluid.36.052203.071431.

A. Toffoli, J. McConochie, M. Ghantous, L. Loffredo, and A. V. Babanin. The effect of wave-induced turbulence on the ocean mixed layer during tropical cylcones: Field observations on the Australian North-West Shelf. *Journal of Geophysical Research*, 117:C00J24, 2012. doi: 10.1029/2011JC007780.

I. B. Troen and L. Mahrt. A simple model of the atmospheric boundary layer; sensitivity to surface evaporation. *Boundary-Layer Meteorology*, 37:129–148, 1986.

L. Umlauf and H. Burchard. A generic length-scale equation for geophysical turbulence models. *Journal of Marine Research*, 61(2):235–265, 2003. ISSN 0022-2402.

L. Umlauf, K. Bolding, and H. Burchard. *GOTM Scientific Documentation. Version 4.2*. 2011. available at http://www.gotm.net/pages/documentation/manual/pdf/a4.pdf.

Fabrice Veron, W. Kendall Melville, and Luc Lenain. Measurements of ocean surface turbulence and wave–turbulence interactions. *Journal of Physical Oceanography*, 39:2310–2323, 2009.

T. von Kármán. Mechanische Ähnlichkeit und Turbulenz. In *Proceedings of the Third International Congress of Applied Mechanics*, Stockholm, 1930.

C. F. von Weizsäcker. Das spektrum der turbulenz bei groen reynoldsschen zahlen. *Zeitschrift für Physik*, 124:614–627, 1948.

Yonggang Wang, Fangli Qiao, Guohong Fang, and Zexun Wei. Application of wave-induced vertical mixing to the K profile parameterization scheme. *Journal of Geophysical Research*, 115(C9):C09014, 2010. doi: 10.1029/2009JC005856.

David C. Wilcox. *Turbulence Modeling for CFD*. DCW Industries, Second edition, 1998.

V. V. Yefimov and G. N. Khristoforov. Spectra and statistical relations between the velocity fluctuations in the upper layer of the sea and surface waves. *Izvestiya, Atmospheric and Oceanic Physics*, 7:1290–1310, 1971a.

V. V. Yefimov and G. N. Khristoforov. Wave-related and turbulent components of velocity spectrum in the top sea layer. *Izvestiya, Atmospheric and Oceanic Physics*, 7:200–211, 1971b.

I. R. Young, A. V. Babanin, and S. Zieger. The decay rate of ocean swell observed by altimeter. *Journal of Physical Oceanography*, 43(11):2322–2333, 2013.

Biao Zhao, Fangli Qiao, and Guansuo Wang. The effects of the non-breaking surface wave-induced vertical mixing on the forecast of tropical cyclone tracks. *Chinese Science Bulletin*, 2014. doi: 10.1007/s11434-014-0255-0.

Malek Ghantous obtained his Ph.D. at the University of Melbourne, studying air-sea interaction. After that he became a research fellow at Swinburne University of Technology, joining what would become the Centre for Ocean Engineering, Science and Technology. There he focused on developing a parameterisation for vertical mixing in the ocean from turbulence generated by wave orbital motion. He is now a post-doctoral fellow at the Laboratoire d'Études en Géophysique et Océanographie Spatiales in Toulouse, working on data assimilation and regional downscaling in an ocean circulation model.

Prof. Alexander W. Babanin was born in Russia where he completed his undergraduate and postgraduate studies before moving to Australia. His Bachelor Degree in Physics and Master Degree in Physical Oceanography come from the six-year course at the Faculty of Physics of the Lomonosov Moscow State University, and his PhD on Spectral Characteristics of Surface Wind Wave Fields from the Marine Hydrophysical Institute in Sebastopol. Since 2004, he works at the Swinburne University of Technology in Melbourne. His research interests involve wind-generated waves, air-sea interaction and ocean turbulence, including dynamics of surface ocean waves, wave breaking and dissipation, air-sea boundary layer, extreme oceanic conditions, wave statistics, ocean mixing, remote sensing.